# Chem Soc Rev

## Supported catalysts based on layered double hydroxides for catalytic oxidation and hydrogenation: general functionality and promising application prospects

SCHOLARONE™
Manuscripts

# Chem.Soc.Rev.

## ARTICLE

# Supported catalysts based on layered double hydroxides for catalytic oxidation and hydrogenation: general functionality and promising application prospects

Junting Feng, Yufei He, Yanan Liu, Yiyun Du, Dianqing Li*

Oxidation and hydrogenation catalysis play a crucial role in the current chemical industry for the production of key chemicals and intermediates. Because of easy separation and recyclability, supported catalysts are widely used in these two processes. Layered double hydroxides (LDHs) with the advantages of unique structure, composition diversity, high stability, ease of preparation and low cost have shown great potential in the design and synthesis of novel supported catalysts. This review summarizes the recent progress in supported catalysts by using LDHs as supports/precursors for catalytic oxidation and hydrogenation. Particularly, partial hydrogenation of acetylene, hydrogenation of dimethyl terephthalate, methanation, epoxidation of olefins, elimination of $NO_x$ and $SO_x$ emissions, and selective oxidation of biomass have been chosen as representative reactions in the petrochemical, fine chemicals, environmental protection and clean energy fields to highlight the potential application and the general functionality of LDH-based catalysts in catalytic oxidation and hydrogenation. Finally, we concisely discuss some of the scientific challenges and opportunities of supported catalysts based on LDH materials.

## 1. Introduction

Catalysis is a crucial technology that affects our everyday life in many ways. Over 90% of all chemical manufacturing is based on, or relies heavily on, catalytic processes.[1] It has been estimated that catalysis could contribute to approximately 35% of the world's gross domestic product (GDP) and the demand for catalysts could reach $19.5 billion in 2016.[2] Among numerous catalytic reactions, oxidation and hydrogenation play a pivotal role in the current chemical industry. Oxidation is the second largest process after polymerization and contributes ~30% of the total output of the chemical industry.[3] A wealth of key chemicals and intermediates such as alcohols, aldehydes, ketones, acids and epoxides are produced via selective oxidation. Catalytic hydrogenation, especially hydrogenation of carbon-carbon multiple bonds and unsaturated aldehydes/ketones, as a fundamental step in the synthesis and manufacture of petrochemicals and fine chemicals has also attracted considerable interest.[4, 5]

Progress in the synthesis of nanoparticles (NPs) has led to materials with extraordinary advantages as compared to their bulk counterparts and has provided opportunities for a potential revolution in the field of catalysis.[6] However, although NPs typically provide highly active centers, they are very small and in a thermodynamically unstable state. Therefore, NPs usually undergo aggregation and suffer from poisoning during reactions, resulting in deactivation and poor reusability.[7] Immobilization of NPs onto a suitable support is potentially one of the most interesting and fruitful ways to solve this problem. Supported catalysts are therefore widely used in industrial-scale oxidation and hydrogenation reactions and have been shown to exhibit good catalytic performance coupled with easy separation and recyclability. There are several factors that influence the catalytic performance of supported catalysts, including the particle size, composition, surface morphology and structure of the active phase, the nature of the support, as well as interaction between the active phase and the support.[8-11] By tuning these parameters, the properties of supported catalysts can, in principle, be tailored to enhance their catalytic performance. However, the design and fabrication of catalysts which can simultaneously satisfy the requirements of high catalytic activity, selectivity and stability is still a long-standing problem in heterogeneous catalysis.

Layered double hydroxides (LDHs), a family of synthetic anionic clays, are a class of two-dimensional (2D) brucite $Mg(OH)_2$-like layered inorganic materials.[12, 13] They can be represented by the general formula $[M^{2+}_{1-x}M^{3+}_x(OH)_2]^{x+}(A^{n-})_{x/n} \cdot mH_2O$, where $M^{2+}$ and $M^{3+}$ represent metallic cations, $A^{n-}$ indicates the interlayer anion, x is the molar ratio of $M^{3+}/(M^{2+}+M^{3+})$ and m represents the amount of water.
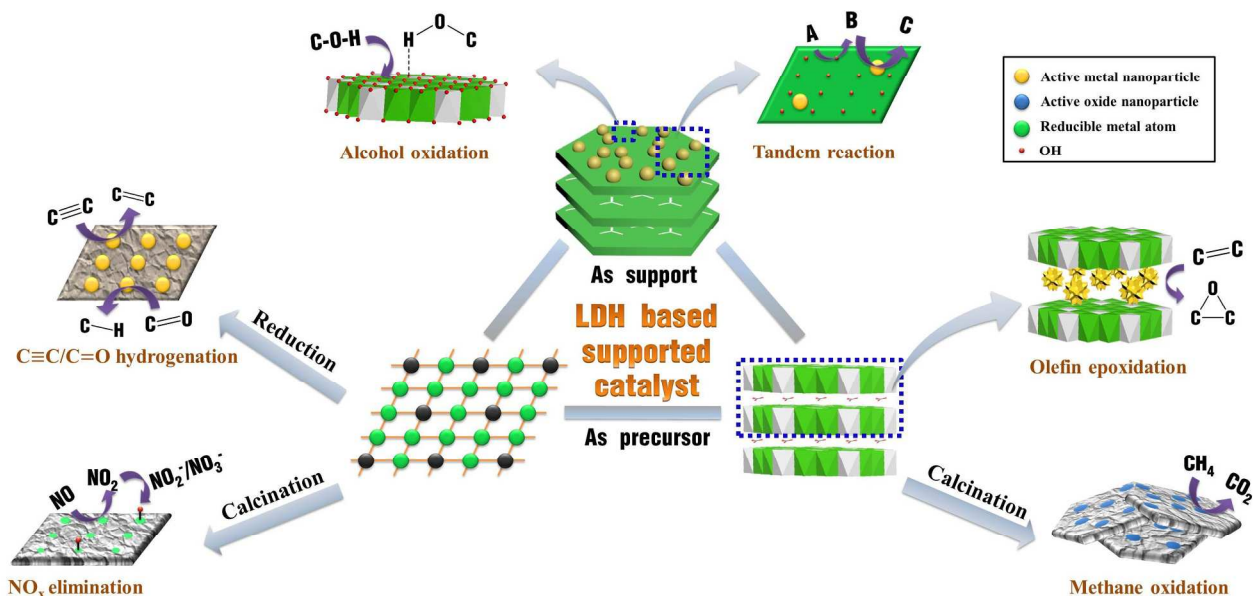
# Chem.Soc.Rev.

## ARTICLE



**Fig.1** Properties and applications of supported catalysts fabricated by using LDHs as supports/precursors for catalytic oxidation and hydrogenation

LDHs are built up by the periodic stacking of positively charged $(M^{2+}, M^{3+})(OH)_6$ octahedral layers and negatively charged interlayer galleries consisting of anions and water.[14, 15] In terms of application in the field of heterogeneous catalysis, LDHs offer a number of advantages: (I) Cation-tunability of the brucite-like layers and anionic exchangeability gives LDHs great versatility in composition;[14, 16] (II) The high adsorption capacity of LDHs themselves—and even more so, the mixed metal oxides (MMO) produced by their calcinations—make them effective supports for the immobilization of catalytically active species on the surface;[17] (III) Tunable basicity of the surface enables LDHs and MMOs to perform as excellent solid base catalysts;[18] (IV) The uniform dispersion of $M^{2+}$ and $M^{3+}$ cations in the layers, as well as preferred orientation of anions in the interlayer, provides opportunities to use LDHs as precursors for the formation of highly and stably dispersed supported catalysts;[19] (V) Combining LDHs with other materials to form hybrid supported catalysts with hierarchical structure offers the benefits of synergistic effects between the two materials and further enhances the catalytic activity and stability.[20] Consequently, the rational design and controllable preparation of supported catalysts based on LDH materials with simultaneously enhanced activity, selectivity and stability is of tremendous interest.

Catalytic applications of LDH materials are being extensively explored, with about 100 papers published each year and some excellent general reviews in the field of catalysis have recently been published by several groups.[17, 21-24] In this review article, we focus on the most recent advances in the synthesis, properties and applications of supported catalysts fabricated by using LDHs and their derivatives as supports or precursors for catalytic oxidation and hydrogenation reactions (Fig. 1). We have chosen these two catalytic reactions because of the rapid developments in fundamental research, as well as their practical importance for the

chemical industry. Some promising application prospects of supported catalysts based on LDHs are highlighted. In addition, comparisons of the different types of reactions are employed to shed light on the structure-performance relationships for these catalysts. Finally, we concisely discuss some of the scientific challenges and opportunities in this field. It is hoped that this review will attract more attention towards supported catalysts based on LDH materials for oxidation and hydrogenation and encourage future work in this exciting area.

## 2. Design and synthesis of supported catalysts based on LDH materials

### 2.1 Utilization of LDHs and MMOs as supports

LDHs and their calcined product MMOs have been shown to be promising supports for the immobilization of various metallic nanoparticles by virtue of their excellent adsorption capacity, the tunable acidity-basicity of the surface, the opportunity to exploit confinement effects and the ease of assembly of the supported catalysts. The possibility of the smart design and controllable synthesis of LDHs with composition, morphology, surface acid-base properties and structure tailored to the demands of a specific catalytic reaction can result in significantly improved catalytic performance.[25, 26]

### 2.1.1 LDH- and MMO-supported catalysts for oxidation

The advantages of LDH materials as supports for metal oxidation catalysts derive from the confinement effect, which ensures small metal particle size and the surface basicity resulting from the abundance of hydroxyl groups on brucite-like layers. The

quantity and strength of basic sites can be controlled by tuning the composition and proportion of cations in LDH layers.[27, 28] With the increasing attention being paid to environmental and economical concerns, LDHs and MMOs have been utilized as environmentally benign and recyclable heterogeneous solid base catalysts to replace conventional homogeneous base catalysts, particularly in liquid phase oxidation processes.[29-31] The surface basicity has been shown to promote the abstraction of protons from organic molecules, especially alcohols, even after metal immobilization.[32]

### 2.1.1.1 Supported Au catalysts for oxidation

Until about 20 years ago, the chemistry of gold was dominated by the perception that gold was non-reactive since in its bulk state it was the most noble of the elements.[33] Recently, much attention has been paid to the development of Au nanoparticle catalysts due to their size-dependent behavior.[34] Kaneda and co-workers[35] reported the formation of small Au NPs with a mean diameter of 2.7 nm on the surface of LDHs to give an MgAl-LDH-supported Au catalyst (Au/LDH), which was found to be reusable as a heterogeneous catalyst for the synthesis of lactones from diols; the catalysts gave a high turnover number (TON) of 1400 in toluene as the solvent using molecular oxygen as an oxidant. The small Au NPs in the Au/LDH catalyst could overcome the problems—such as the requirements for high temperatures, additives and high catalyst loading—that have plagued previously reported lactonization catalyst systems. The same authors further investigated the catalytic performance of LDH-supported Au NPs for the aerobic oxidation of alcohols under mild reaction conditions.[36] Compared with the same catalysts loaded on other oxide supports ($MgO$, $Al_2O_3$, $TiO_2$ and $SiO_2$), the TON and turnover frequency (TOF) of Au/LDHs were significantly higher, reaching values as high as 200,000 and 8,300 h$^{-1}$, respectively, in the oxidation of neat 1-phenylethanol. Moreover, the Au/LDH catalyst could be reused in three consecutive runs without any loss of activity and selectivity. The excellent catalytic properties of Au/LDHs in the aerobic oxidation of secondary alcohols have also been reported.[37] X-ray photoelectron spectroscopy (XPS) showed that, compared with Au/TiO$_2$ and Au/SiO$_2$, the Au 4f$_{7/2}$ peak of the Au NPs was shifted to lower binding energy after immobilizing on the LDH support, indicating that the Au NPs were adsorbed as negatively charged species, consistent with the positive charge on the LDH layers. It was known that negatively charged Au nanoparticles enhance the activation of molecular oxygen in the aerobic oxidation of alcohols accounting for the superior performance on Au/LDHs compared to the same Au NPs on other supports.

Furthermore, the performance of the Au/LDH catalysts can be tailored by simply adjusting the basicity of the LDH support by variation of the Mg/Al atomic ratio. Liu and co-workers[38] prepared a series of LDH supports with Mg/Al atomic ratio varying from 2 to 6 and found that the Mg/Al atomic ratio of the LDH strongly affected the catalytic performance of the material in aerobic alcohol oxidation, the tandem oxidative esterification of alcohols to methyl esters, the tandem oxidative coupling of alcohols and amines to imines. For example, the maximum yield of benzaldehyde in the aerobic oxidation of benzyl alcohol was observed for an Au/Mg$_3$Al-LDH catalyst. When using a higher Mg/Al ratio, they found that the resulting Au/Mg$_5$Al-LDH catalyst could almost quantitatively convert benzyl alcohol into methyl benzoate by tandem oxidative coupling of alcohols. Both the activity and ester selectivity of the Au/Mg$_x$Al-LDH catalysts generally increased with increasing Mg/Al ratio. However, the catalytic properties of Au/Mg$_6$Al-LDH were poorer, due to its poor activity in alcohol

oxidation which was the slow step in the tandem reaction. In the case of oxidative tandem synthesis of imines, Au/Mg$_2$Al-LDH—with moderate basicity—showed the best catalytic performance, with imine selectivities of up to 97%. It was because the moderate basicity favored the reaction of an aldehyde with an amine to form an imine, whereas this reaction was unfavorable with strongly basic catalysts. The calcination temperature used in the synthesis of Au$^0$ species supported on the LDH was also found to be important. The Au$^{3+}$ precursor, believed to be a cationic $\{[Au(NH_3)_2(H_2O)_{2-x}(OH)_x]^{(3-x)}\}^+$ complex, underwent a gradual reduction to Au metal on increasing the calcination temperature, since the temperature affected the thermodynamic equilibrium.[39] For example, a material prepared by calcination below 323 K showed no catalytic activity for the oxidation of glycerol, whereas catalysts prepared by calcination at temperatures higher than 373 K exhibited high glycerol conversion (over 70%). Furthermore, the wide range of M$^{2+}$ and M$^{3+}$ (and even M$^{4+}$) cations which can be incorporated in the LDH layers provides the possibility of improving the performance of an LDH-supported catalyst by optimizing the interaction between the support and the active component. For example, MAl-LDH (M = Mg, Ni, Co)-supported catalysts containing Au nanoclusters (AuNCs) with an average size of 1.5 nm were synthesized using by taking advantage of the strong interactions between the anionic glutathione-capped AuNC precursor (GS-AuNCs) and the cationic layers of MAl-LDH (Fig. 2).[40] After calcinations to remove the glutathione ligands, the resulting Au/NiAl-LDH catalyst exhibited excellent catalytic performance in the oxidation of 1-phenylethanol in toluene, with a TOF of 46500 h$^{-1}$, without the need for any basic additives. It was suggested that the presence of transition metal cations in the LDH support enhanced the Au-support synergistic effect, which led to an increase in the catalytic performance. Very recently, Li et al.[41] reported a novel Au catalyst supported on flower-like NiAl-LDH with hierarchical pore structure and also revealed the synergy between Au and support. Compared with that of the common Au/NiAl-LDH catalyst, the activity of the flower-like catalyst was dramatically enhanced by 60% due to the confinement effect of the hierarchical pores which increased the effective collisions between substrates and active sites in the oxidation of benzyl alcohol in toluene.
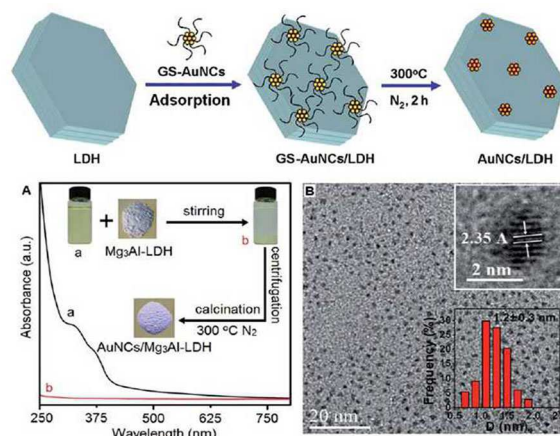


**Fig. 2** Schematic of the AuNCs/LDH catalyst and (A) UV-vis spectra of the original solution of GS-AuNCs (a) and the supernatant after impregnation over LDH (using Mg$_3$Al-LDH as the example) (b); (B) HRTEM image of GS-AuNCs (inset shows the crystalline structure of an individual NC and the histogram of the size distribution) Reproduced from ref. 40. Copyright 2014 The Royal Society of Chemistry.

Similarly, Liu et al.[42] combined Au NPs with a MgCr-LDH support to obtain a highly efficient heterogeneous Au/LDH catalyst

for aerobic alcohol oxidation. The extent of Au-support synergy enhanced with the decreasing size of Au NPs and increasing Cr content. The strong Au-support synergy was related to a $Cr^{3+}$-$Cr^{6+}$ redox cycle occurring at the Au/support interface, where $O_2$ activation took place accompanied by electron transfer from LDH to Au NPs. The interfacial $Cr^{6+}$ species were then reduced by surface Au-H hydride and negatively-charged Au species. The enhanced Au-LDH interactions accordingly increased the rate of $O_2$ activation and O-H bond cleavage (Fig. 3).
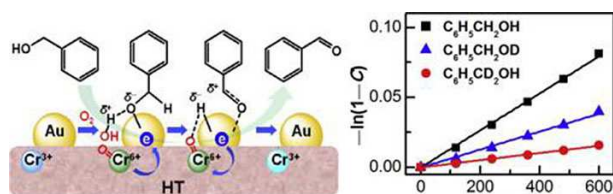


**Fig. 3** The proposed mechanism for the efficient aerobic oxidation of alcohols on a heterogeneous Au/MgCr-LDH catalyst. Reproduced from ref. 42. Copyright 2014 Elsevier.

An example of the confinement effect afforded by LDH supports was reported by Li and co-workers.[43] A flocculation and in situ reduction method was employed to synthesize an Au/LDH catalyst. In this composite, Au NPs were evenly dispersed in MgAl-LDH interlayer gallery and the particle size of the Au NPs was thus restricted to less than 1 nm. The highly dispersed Au/LDH catalyst exhibited excellent performance in low temperature CO oxidation, which could be initiated at temperatures lower than -30 $^o$C.

In order to extend the practical applications of LDH materials in the field of catalytic oxidation, their hybridization with specific functional materials to afford hierarchically structured nanocomposites has attracted extensive attention. The resulting materials can possess not only enhanced activity and selectivity resulting from the synergy between two materials, but also improved stability and recyclability by virtue of the structured architecture.[44, 45] Thus, development of LDH hybrid composites is of high interest in terms of both fundamental research and practical industrial applications. For example, magnetically separable nanocatalysts have attracted increasing interest in recent years owing to the convenient separation of the catalyst from a substrate by an external magnetic field. However, directly coating reactive nanoparticles onto a magnetic core such as $Fe_3O_4$ was not very effective due to either a lack of linkage groups,[46] or an unfavorable heterojunction between the coating layer and the iron oxide core resulting from the post-treatment necessary to crystallize the NPs.[47] Therefore, core@shell type three-phase composites—hierarchical composites with a magnetic core and an LDH shell structure loaded with the active catalyst—were preferable. One example of a simple synthesis of a novel core-shell structure $Fe_3O_4$@MgAl-LDH@Au catalyst is shown in Fig. 4.[48] There were two key steps in the synthesis process. First, a surfactant-free solvothermal method was employed to prepare a monodisperse magnetite $Fe_3O_4$@MgAl-LDH precursor. Au NPs were then immobilized on the precursor by a deposition-precipitation (DP) method. When employed in the catalytic oxidation of 1-phenylethanol, this catalyst yielded 99% acetophenone with a TOF of 66 h$^{-1}$. This excellent activity could be attributed to both the alkalinity of the LDH surface and the honeycomb-like morphology resulting from the vertical orientation of LDH platelets (i.e. perpendicular to the surface of the substrate) which facilitated the collision between the active catalyst and substrate. Moreover, since the AuNPs were separated by interleaving between LDH platelets, this prevented aggregation of the particles and, as a result, no deactivation was observed in five consecutive reaction cycles.
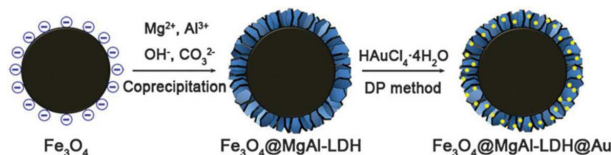


**Fig. 4** The synthetic strategy for an $Fe_3O_4$@MgAl-LDH@Au catalyst. Reproduced from ref. 48. Copyright 2011 The Royal Society of Chemistry.
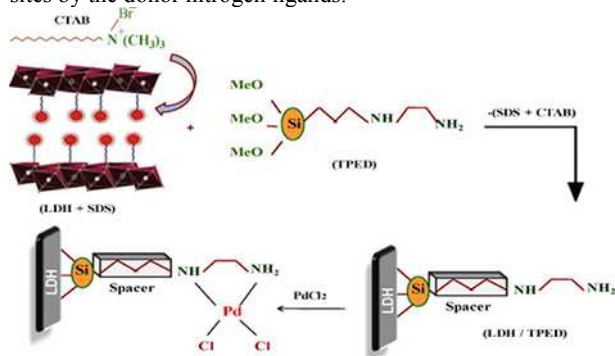
**2.1.1.2 Supported Pd catalysts for oxidation**

In 2000, an MgAl-LDH-grafted Pd(II) heterogeneous catalyst species (Pd/LDH) was prepared from commercially available reagents by Uemura's group.[49] LDH was found to be superior to several other clays when used as a support for Pd(II) in the oxidation of alcohols by oxygen. Particularly noteworthy was that in the oxidation of allylic alcohols such as geraniol and nerol which were prone to geometric isomerization, the corresponding aldehydes were obtained in high yield without any isomerization. In addition, the Pd/LDH catalyst can be easily separated and recycled. For the purpose of constructing a "greener" oxidation system, the authors further investigated the Pd/LDH catalyzed oxidation of a variety of primary and secondary alcohols to the corresponding aldehydes and ketones in toluene using an atmospheric pressure of air as the sole oxidant instead of pure molecular oxygen. High yields were obtained over the Pd/LDH catalyst and the results were quite similar to those obtained using molecular oxygen.[50]

By taking advantage of the Brønsted basic sites on LDHs, Chen et al.[51] prepared a multifunctional catalyst by immobilizing Pd NPs on the surface of an MgAl-LDH for use in the solvent-free oxidation of benzyl alcohol. They found that the layered structure of the LDH could be reconstructed to different extents by calcination and rehydration in ethanol aqueous solution under different conditions, which afforded varying numbers of Brønsted basic sites. The catalyst with the largest amount of Brønsted basic sites was most active for the oxidation of benzyl alcohol and the excellent yield of benzaldehyde was maintained after five runs. They suggested that the Brønsted basic sites on the LDH support facilitated β-H elimination from the metal alkoxide intermediate, thus leading to strong enhancement of the activity of the supported Pd particles in benzyl alcohol oxidation. Moreover, the calcination imposed a restricted nano-size on the supported Pd particles unlike the reduction with hydrazine hydrate, which provided a convenient approach to control the size of Pd NPs on the LDH surface. Li and co-workers[52] synthesized a series of Pd/$Co_3$:Al spinel catalysts using CoAl-LDHs as the precursor of the support and investigated the structure-property relationships for these materials when used as catalysts for the total oxidation of toluene. The CoAl-LDH precursors were prepared the by co-precipitation method and the Pd active species were introduced by a variety of different approaches, including impregnation, wet ion-exchange and during the direct co-precipitation stage (COP). It was found that the Pd/Pd/$Co_3$:Al spinel (COP) catalyst was more active than both the other LDH-derived catalysts and the catalyst prepared by a traditional thermal combustion method. This superior catalytic activity could be attributed to the improved Pd dispersion, redox characteristics and oxygen vacancies. The Pd/$Co_3$:Al spinel (COP) catalyst possessed the largest Brunauer-Emmett-Teller surface area ($S_{BET}$ = 93 m$^2$/g), while having the smallest mean crystallite size of $Co_3$:Al spinel (11.6 nm). The palladium content on the surface of Pd/$Co_3$:Al spinel catalyst (COP) (as determined by XPS) was close to the bulk value (1.0 wt.%), indicating that the distribution of palladium species was relatively homogeneous throughout. Moreover, a

synergistic effect between PdO and $Co_3O_4$ in the Pd/$Co_3$:Al spinel (COP) catalyst due to the strong reducibility of PdO and $Co_3O_4$ as well as rich oxygen vacancies on the $Co_3$:Al spinel surface also contributed to the enhanced activity.

Sahoo and Parida synthesized a heterogeneous and recyclable Pd(II) catalyst supported on a diamine-functionalized ZnAl-LDH and for use in the oxidation of primary alcohols.[53] The synthesis of the Pd(II)/LDH catalyst is illustrated in Fig. 5. NMR spectroscopy confirmed that the ligand N-[3-(trimethoxysilyl)-propyl] ethenediamine (TPED) was covalently attached to the surface of the LDH and the formation of N-Pd coordinate bonds was confirmed by XPS. Oxidation of benzyl alcohol over this catalyst afforded 94% conversion of benzaldehyde with 100% selectivity for benzaldehyde. Substituted benzyl alcohols with either electron-donating or electron-withdrawing substituents in the benzene ring were all found to be less reactive than benzyl alcohol. The heterogeneous catalyst can be easily recovered and reused multiple times without any significant loss of catalytic activity and selectivity; this was ascribed to the stabilization of the active Pd sites by the donor nitrogen ligands.



**Fig. 5** Schematic pathway for the synthesis of a Pd(II)/LDH catalyst. Reproduced from ref. 53. Copyright 2013 Elsevier.

### 2.1.1.3 Supported Ru catalysts for oxidation

LDH-supported Ru catalysts have been used not only in the aerobic oxidation of alcohols, but also in a tandem reaction as bifunctional catalysts. Kaneda's group prepared a ruthenium-grafted LDH (Ru/LDH) by treating an MgAl-LDH with the required basicity with aqueous $RuCl_3 \cdot nH_2O$ using a surface impregnation method.[54] The structure of the Ru species on LDH surface was analyzed by Ru K-edge X-ray-absorption fine-structure spectroscopy (XAFS). The X-ray absorption near-edge structure (XANES) spectrum of the Ru/LDH was similar to that of $Ru(IV)O_2$ but differed from that of $Ru(III)(acac)_3$, indicating that the Ru species was in the +4 oxidation state. The extended X-ray absorption fine structure (EXAFS) analysis suggested a monomeric Ru(IV) species having one hydroxyl ligand and two water ligands grafted on a triad of oxygen atoms on the surface of the LDH. The Ru/LDH catalyst was shown to effectively promote α-alkylation reactions of various nitriles with primary alcohols or carbonyl compounds through tandem reactions consisting of metal-catalyzed oxidation and reduction and an aldol reaction promoted by the basic sites present onto LDH.

The quinoline nucleus plays an important role as an intermediate in the design of pharmacologically active compounds. Generally, the direct formation of quinolines from 2-aminobenzyl alcohol and ketones involves a hydrogen transfer reaction and cyclization mediated by a homogeneous Ru complex catalyst system with a stoichiometric amount of KOH.[55,56] Kaneda's group first reported tandem quinoline synthesis using heterogeneous Ru/LDH catalysts without the need for homogeneous bases. In this reaction system,

quinolines were obtained through aerobic oxidation catalyzed by the Ru species, followed by an aldol reaction on basic sites of the LDHs. [57]

### 2.1.1.4 Supported Pt catalysts for oxidation

Driven by the need to develop alternatives to non-renewable resources, C5 and C6 sugars derived from agricultural waste are increasingly being explored as feedstocks for the chemical industry. Oxidation is a key step in converting these precursors to more valuable materials. For examples, glucose derived from cellulose can be used as a food additive but it can also be converted to high added value gluconic and glucaric acid through selective oxidation. Dhepe's group compared an acidic material ($Al_2O_3$) and a basic material (MgAl-MMO) as supports for Pt catalysts for use in the oxidation of glucose and xylose.[58] They found that an 83% yield of gluconic acid and a 57% yield of xylonic acid were achieved over Pt/MMO catalyst in the absence of a homogeneous base. Comparison with acid support, using a basic support like an MMO as a replacement for a homogeneous base in oxidation reactions made the entire process environmentally benign and safe. UV spectroscopy showed that the sugars preferentially remained in the open chain form in the presence of an MMO and thus the exposed CHO groups were able to undergo oxidation reactions to yield acids. In addition, the strong interaction between Pt and the MMO support also contributed to the excellent activity.

### 2.1.1.5 Supported bimetallic catalyst for oxidation

Recently, MgAl-MMO was used as support to prepare highly efficient and reusable bimetallic PdAu catalysts by using sol-immobilization method for the solvent-free oxidation of benzyl alcohol.[59] During the immobilization step, MgAl-MMO support spontaneously reconstructed to their origin form MgAl-LDH. Therefore, the obtained catalyst was in the form of PdAu/MgAl-LDH. Compared with the monometallic Pd and Au catalysts on the same support, LDH-supported AuPd catalysts showed an increase in both activity and selectivity for benzaldehyde and, moreover, an improved resistance to catalyst deactivation. The bifunctional acid-base nature of the LDH support was shown to be important in this catalytic process: the acid sites were considered to be responsible for the improvement in catalytic activity, while the basic sites enhanced the selectivity towards benzaldehyde. The TON for the $Au_1Pd_1$/LDH catalyst was 13 000 after 4 h and the selectivity to benzaldehyde was maintained at 93% even after three consecutive runs. Based on the experimental results and previous findings, a possible mechanism involved was proposed (Fig. 6), whereby the oxidation of benzyl alcohol proceeded through the cooperation between the AuPd nanoalloys and the acid-base sites on the surface of the LDH support. In the first step, a basic $MgOH^{\delta-}$ site on the support abstracted a proton from benzyl alcohol to give an alkoxide intermediate coordinated at the interface with elimination of a water molecule. In the second step, the alkoxide intermediate formed a metal-H bond with the coordinately unsaturated active AuPd species to afford an unstable AuPd-alkoxide-LDH species, followed by β-hydride elimination to give a metal hydride species together with the corresponding carbonyl compound. Finally, the metal hydride was rapidly oxidized to form water promoted by the acid sites of the support, with concomitant recovery of the initial AuPd metallic site, thereby completing the catalytic cycle.
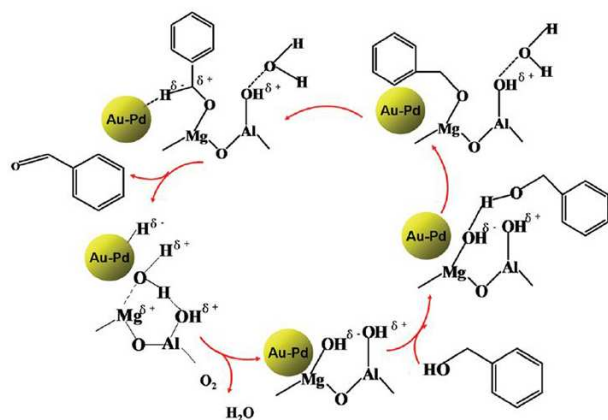
**Fig. 6** A possible reaction pathway for the solvent free oxidation of benzyl alcohol over an AuPd/MgAl-LDH catalyst. Reproduced from ref. 59. Copyright 2013 The Royal Society of Chemistry.

#### 2.1.1.6 Other LDH- and MMO-supported catalysts for oxidation

As outlined above, metals immobilized on both LDHs and MMOs can act as efficient heterogeneous catalysts for a variety of oxidation reactions. XAFS showed that high-valent Mn species (with an average oxidation state of +6) could be created on an MgAl-LDH surface by oxidation of $Mn^{2+}$ using aqueous KOH.[60] Smooth and reversible interconversion between low- and high-valent cationic Mn species enabled the oxidation of benzyl alcohols to the corresponding carbonyl compounds using molecular oxygen at 100 °C in toluene solvent. The authors subsequently investigated the catalytic activity of the material for the oxidation of other alcohols. A high catalytic activity was observed for the oxidation of benzylic alcohols with functional groups such as chloro, nitro and methyl at the *para* positions, as well as heterocyclic alcohols. In addition, cinnamyl alcohol resulted in the corresponding cinnamaldehyde with preservation of the C=C double bond. However, low yields of products were observed for the oxidation of aliphatic and allylic alcohols such as 2-octanol and geraniol. Reddy and co-workers[61] reported a heterogeneous $OsO_4$/MgAl-LDH catalyst for the asymmetric oxidation of sulfides to sulfoxides using *N*-methylmorpholine *N*-oxide as co-oxidant. Importantly, this catalyst could be reused for three cycles with only a slight loss of activity.

Although they can show high activity, the use of LDH catalysts in the powdered form presents problems in terms of large scale application in industry because of large bed pressure drops and mass/heat transfer resistance, as well as difficulty in recycling. A approach which was attracting considerable attention was to grow an LDH support on aluminum foil, since this afforded a structured catalyst with excellent mass flow properties and recyclability, as well as high thermal conductivity, which could dissipate heat generated in an exothermic reaction. Moreover, the oriented growth of LDH on the aluminium surface led to the formation of linear macropores and a uniform pore size distribution. In addition, these LDHs could be calcined to afford MMOs which remained firmly anchored on the aluminium foil surface. Wei et al. reported structured catalysts formed by immobilizing cobalt phthalocyanine tetrasulfonate (CoPcS) on the hybrid film materials MgNiAl-MMO/Al foil[62] and MgCoAl-MMO/Al foil[63] for mercaptan sweetening (the oxidation of mercaptans to disulfides), an important process in the petrochemical industry. These membrane catalysts demonstrated convenient manipulation and high catalytic performance, which was attributed not only to the above-mentioned

advantages, but also to the abundance of moderate basic sites and high dispersion of the active phase. In a similar way, Kovanda and coworkers[64] fabricated a Co-Mn-Al MMO catalyst supported on anodized aluminum foil for use in ethanol oxidation. However, it was worth noting that the melting point of aluminium foil is only 660 °C, which became the main constraint on its development, especially for use in high-temperature reactions.

#### 2.1.2 LDH- and MMO-supported catalysts for hydrogenation

In addition to their application in oxidation reactions, LDH-supported metallic catalysts are also widely used as hydrogenation catalysts, particularly for the hydrogenation of unsaturated C-C and C-O bonds, nitro compounds and in coupling reactions.[65-68]

#### 2.1.2.1 Supported Pd catalysts for hydrogenation

LDHs and MMOs are attractive alternatives to conventional supports for Pd hydrogenation catalysts—such as active carbon, zeolites, $SiO_2$, $Al_2O_3$ and MgO—because the basic properties of the support can endow LDH or MMO-supported Pd catalysts with unusual properties. Sangeetha and co-workers[69] reported the preparation of 1 wt.% Pd supported on MgAl-MMO, MgO and γ-$Al_2O_3$ catalysts using a wet impregnation method for use in the vapor phase hydrogenation of nitrobenzene. The conversion of nitrobenzene was studied in the temperature region 498-573 K and a significantly higher activity was observed over the Pd/MMO catalyst when compared with the other two catalysts. The superior catalytic performance was attributed to the small particle size and high degree of dispersion of the Pd particles on the MMO support. TEM images showed that Pd particles with average size of 1.6 nm were evenly distributed on the surface of the MMO, whereas large Pd particles and agglomerates were found in Pd/$Al_2O_3$ and Pd/MgO. The high degree of dispersion of Pd on the surface of the MMO was confirmed by CO chemisorption measurements. It was suggested that Pd atoms were firmly anchored on the support owing to the basicity of the MMO, which reduced the possibility of agglomeration or aggregation of Pd on the MMO surface. Similarly, Padmasri et al.[70] investigated the effect of the support for Pd catalysts used in the selective hydrodechlorination of $CCl_2F_2$ to $CH_2F_2$. A Pd/MgAl-MMO catalyst was found to be superior to the corresponding oxides, viz., MgO, γ-$Al_2O_3$ supported Pd catalysts in terms of both activity and selectivity towards $CH_2F_2$. The enhanced activity over the Pd/MgAl-MMO catalyst was attributed to the high Pd dispersion, while the superior selectivity might be related to the increased acidity of the catalyst after reduction, which maintained the Pd sites in an electron deficient environment.

Tichit's group[71] performed semi-hydrogenation of 2-butyne-1,4-diol with MgAl-MMO-supported Pd catalysts prepared by three different routes: impregnation, co-precipitation and anionic exchange. The highest TOF (20.6 s⁻¹) was observed over Pd/MMO prepared by the impregnation method, since the small Pd particles were involved in a strong interaction with the support. The promotion of the small Pd particles by the ''electron donor'' support decreased the energy of adsorption of the unsaturated species and markedly improved the hydrogenation rate of C≡C bonds. In this reaction butan-1-ol was the only by-product, which was attributed to the acid sites on MMO surface, since it resulted from the hydrogenation and dehydration of the γ-hydroxybutyraldehyde intermediate obtained by isomerisation of 2-butene-1,4-diol on the acid sites. Sangeetha et al.[72] studied the effect of the support used with Pd catalysts for the conversion of nitrobenzene to aniline. They found that a Pd/MgAl-MMO catalyst

was more active than MgO and γ-Al$_2$O$_3$ supported Pd catalysts, which was attributed to the presence of a larger number of finely dispersed Pd particles on the support.

The catalytic efficiency of Pd/LDH catalysts can be further improved by surface modification. Liu and co-workers prepared Pd/MgAl-LDH catalysts by immobilizing Pd$^{2+}$ on LDH by means of an amino acid, arginine, followed by reduction with NaBH$_4$ at room temperature.[73] XPS and HRTEM results showed that the Pd mainly existed in the form of Pd$^0$ and was distributed uniformly on the support with a mean particle size of 4 nm. The resulting Arg-Pd/LDH catalysts were then used to catalyze the transfer hydrogenation of aromatic ketones. The conversion of acetophenone over Arg-Pd/LDH reached 97.0% in 6 h and the TOF reached 37.7 h$^{-1}$, values which were much higher than those for the corresponding Pd/LDH catalyst without modification by arginine (and those of other previously reported heterogeneous catalysts). The high catalytic activity was attributed to the strong synergistic effect between Pd NPs and Arg-LDH: the amino groups in arginine not only assisted the loading of Pd NPs on the LDH via a combination of strong electrostatic interactions and coordination between NH$_2$-containing ligands and Pd species, but also formed hydrogen bonds with isopropanol which promoted the transfer hydrogenation of acetophenone. There was almost no activity loss after the catalyst was reused five times, suggesting that the as-obtained catalyst was rather stable. This excellent stability could result from the strong interaction between Pd particles and arginine. Specifically, the guanidyl group in arginine formed a coordination complex with the Pd$^{2+}$ precursor and further acted as a stabilizing agent for Pd NPs after the Pd$^{2+}$ species were reduced. In addition, Li et al. have reported a series of LDH-supported Pd catalysts and investigated their catalytic performance and structure-property relationships in the partial hydrogenation of acetylene and these will be reviewed in Section 3.[74-77]

Owing to the acid-basic character of LDHs and high catalytic activity of Pd in hydrogenation reactions, LDH and MMO supported Pd catalysts have also been used as multifunctional catalysts for the tandem synthesis of valuable organic compounds.[78] The condensation and selective hydrogenation of acetone to methyl isobutyl ketone (MIBK) was studied over a series of 0.1-1.5 wt.% Pd/MgAl-MMO catalysts in a liquid-phase batch microreactor. The first step of this tandem reaction was the self-condensation of acetone to diacetone alcohol (DAA), followed by the dehydration of DAA to mesityl oxide (MO). The intermediate, MO, was then selectively hydrogenated at the C=C bond to form MIBK. The parent MMO (without Pd) could catalyze the condensation of acetone and the subsequent dehydration process. Only traces of MIBK were produced, due to the lack of a hydrogenation catalyst. The maximum selectivity to MO was ca. 85%, which was directly related to the optimal acidity and basicity of MMO. As expected, higher acetone conversion (38.0%) and selectivity to MIBK (82.2%) were achieved over Pd/MMO. Additionally, a monotonic decrease in acetone conversion as well as decreased selectivity to DAA and MIBK with increasing metal loading was observed. A 0.1 wt.% metal loading was found to be sufficient to fully hydrogenate MO to MIBK, which was not the rate-determining step and could minimize acetone hydrogenation to isopropanol. It was suggested that the presence of acid and base sites was responsible for the condensation reaction and the Pd sites for hydrogenation step. Although both must be present in order to form MIBK, they did not need to be physically adjacent. Winter et al.[79] evaluated a Pd/MgAl-MMO catalyst and physical mixture of Pd/C and the same MMO catalyst in the tandem synthesis of MIBK. The rate of the dehydration reaction was found to be dependent on the number of strong basic sites and a dependence on

Pd loading was found for the yield of MIBK over the Pd/MMO catalyst. In contrast the activity of the physically mixed catalyst was independent of Pd loading over the same range. The dependence of the activity of the Pd/MMO catalyst on Pd loading was explained in terms of the entrapment of Pd particles in the agglomerates of the irregular stacks of MMO platelets, which made some of the Pd sites inaccessible to the reactants.

A Pd/MgAl-LDH catalyst was also employed in the one-pot synthesis of α-alkylated nitriles, which were important building blocks for various biologically active compounds. This tandem synthesis was performed with carbonyl compounds involving an aldol condensation and hydrogenation reactions. Compared with other basic supports, the LDH-supported Pd catalyst—and even the pristine LDH support—showed a high performance in the aldol reaction, affording (E)-ethyl 2-cyano-3-phenyl-2-propenoate. After the aldol condensation, a high yield of ethyl 2-cyano-3-phenylpropanoate was achieved over Pd/LDH catalyst under an H$_2$ atmosphere Interestingly, the catalytic activity of the Pd/LDH catalyst for the hydrogenation reaction was superior to that of a commercially available Pd/C catalyst.[80] Tichit's group evaluated the potential of Pd/MgAl-MMO catalysts prepared by three different methods in the tandem synthesis of 2-methyl-3-phenyl-propanal (MPPAL) from benzaldehyde and propanal.[81] As shown in Fig. 7, the full process involved two steps: condensation and dehydration carried out in an N$_2$ atmosphere, followed by hydrogenation with H$_2$. The activity of the catalysts in the first stage was related to the reconstruction ability of MMO —the LDH was calcined to MMO and then reconstructed to give an activated LDH in the propanol/water solvent and therefore presenting Brønsted basic sites, while, the hydrogenation ability could be correlated with the Pd particle size. The hydrogenation activity showed an inverse relationship with the particle size, which was ascribed to the decreased adsorption strength of the C=C bond due to the enhancement of the metal-support interaction for larger Pd particles. 77% selectivity for MPPAL was achieved over a Pd/Mg(Al)O catalyst prepared by the anionic exchange method at 64% benzaldehyde conversion. Moreover, the addition of water to the reaction medium improved the conversion of benzaldehyde and prevented the Meerwein-Pondorf-Verley reaction between benzaldehyde and 1-propanol from occurring on the Lewis basic sites of the Mg(Al)O mixed oxide which resulted in the reconstruction of the catalysts to afford an LDH structure containing Brønsted basic sites.
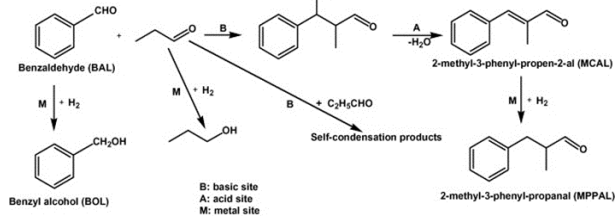


**Fig.7** Simplified scheme for the reaction of benzaldehyde and propanal in N$_2$ and/or H$_2$ atmospheres. Reproduced from ref. 81. Copyright 2007 Elsevier.

### 2.1.2.2 Supported Pt catalysts for hydrogenation

LDH-supported Pt NPs are also highly selective and stable catalysts for hydrogenation reactions. Recently, Xiang and co-workers synthesized Pt/MgAl-LDH catalysts by an environmentally benign solution chemistry method using sucrose as a reducing agent mediated by a tetradecyltrimethylammonium bromide surfactant. The size of the Pt particles could be finely

controlled by varying the ratio of surfactant to metal precursor. [82] When used as a catalyst for the selective hydrogenation of cinnamaldehyde, the as-synthesized Pt/LDH catalyst with a particle size of 5.0 nm showed the highest activity (TOF 0.488 s⁻¹) and selectivity toward cinnamyl alcohol (85.4%). This excellent catalytic performance was attributed to both the particle size and the nature of the support. Decreasing Pt particle size increased the catalytic activity, but resulted in a dramatic drop in selectivity to cinnamyl alcohol. In addition, the hydroxyl groups on the LDH inhibited the adsorption of the C=C bond by electrostatically repelling the phenyl ring of cinnamaldehyde, whilst the hydrophilicity of the LDH had a beneficial effect on the orientation of the hydrophilic C=O moiety on the active site of the catalyst. Dhepe's group employed a Pt/MgAl-MMO catalyst in the hydrogenation reaction of sugars to form the corresponding alcohols. [58] In the hydrogenation of glucose at 90 ᵒC using 16 bar hydrogen pressure, Pt/MMO showed 39% sugar alcohol yield (80% conversion). Under the same conditions, much lower activity was observed for a Pt/γ-Al$_2$O$_3$ catalyst (8.4% yield, 15% conversion) and apart from C6-sugar alcohol, the formation of C5-sugar alcohol (xylitol), 1,2-ethanediol, 1,2-propanediol, glycerol, gluconic acid and levulinic acid was observed as well. The results clearly indicated that the Pt/MMO catalytic system gave superior yield of C6-sugar alcohols compared to Pt/γ-Al$_2$O$_3$ catalysts. Similarly, the Pt/MMO catalytic system showed better activity (50% yield with 59% conversion) than that of Pt/Al$_2$O$_3$ in the hydrogenation of xylose. [58] There were two reasons for the superiority of Pt/MMO compared with the Pt/Al$_2$O$_3$ catalyst: an abundance of hydrogen ions on the MMO support owing to the separation effect of O²⁻-metal cation pairs in the support which were available for the hydrogenation reaction and the Strong Metal-Support Interaction (SMSI) in Pt/MMO, which was less marked in the Pt/γ-Al$_2$O$_3$ catalyst. A Pt/MgAl-MMO catalyst was also employed in the one-pot synthesis of MIBK, with the by-products with Pt/MMO catalyst being quite different from those with a Pd/MMO catalyst: Pt/MMO was more selective for the direct hydrogenation to isopropanol, while Pd/MMO produced more of the diacetone alcohol intermediate. [78]

### 2.1.2.3 Other LDH- and MMO-supported catalysts for hydrogenation

As an alternative to LDH-supported noble metal catalysts, Co/LDHs can also be used as hydrogenation catalysts. For example, Tsai et al. [83] reported the use of Co catalysts supported on MgAl-LDHs for CO hydrogenation. Their work focused on the catalytic activity of the Co/LDH catalyst and the role of the support in the reaction. It was found that the Co/LDH catalyst showed a higher steady-state reaction rate compared with MgO, Al$_2$O$_3$ and MMO (LDH pre-calcined at 500 ᵒC) supported Co catalyst and better product selectivity than Co/Al$_2$O$_3$. Co/Al$_2$O$_3$ catalysts modified with Ru or Re have been reported to possess excellent catalytic performance for Fischer-Tropsch synthesis (FTS). [84] However, when LDHs were used as the support for the cobalt catalyst, it was found to have the ability to increase the reaction rate without the need for a second metal as a reduction promoter. [85] The high FTS activity and selectivity to C5-C7 hydrocarbons over Co/LDH was attributed to the high Co dispersion and the low reducibility and optimum basicity of the LDH.

Albertazzi and co-workers[86] synthesized bimetallic Pd/Pt catalysts supported on basic Mg/Al mixed oxide obtained by calcination of a commercial MgAl-LDH in the vapor-phase hydrogenation of naphthalene in order to investigate the role of the Pd/Pt active phase and the acidity of the support on the

hydrogenolysis/ring-opening reaction, as well as the thio-tolerance of the catalysts. They claimed that the high surface area and the regularly rough surface achieved after calcination of the LDH facilitated the anchoring of the Pd/Pt active phase. Additionally, the acid sites of the support were responsible for both the ring-opening reactions leading to the desired high molecular weight compounds, as well as the cracking reactions giving useless low molecular weight products. The best compromise between hydrogenation (decalin) and hydrogenolysis (high molecular weight products) activity was observed for a Pd/Pt (atomic ratio = 4)/MMO catalyst. Due to the absence of strong Brønsted acid sites, high hydrogenation activity was achieved, while no useless low molecular weight cracking and/or heavy compounds were formed over the optimal catalysts. In addition, in an atmosphere with a relatively high concentration of dibenzothiophene, no obvious loss of activity was observed. This surprising result highlighted the intrinsic thio-tolerance of the Pd/Pt pair and the key role of the acid sites on the MMO surface.

### 2.2 Utilization of LDHs as precursors of supported catalysts

Generally, supported catalysts prepared by the conventional impregnation method often suffer from an inhomogeneity in the distribution of active components over the support due to the surface tension of the impregnating solution. Moreover, the weak interactions between the support and active phase lead to the migration and aggregation of metal particles during the subsequent reduction process and when used in catalytic reactions. [87] As an alternative approach, the sol-immobilization method offers opportunities to minimize the formation of larger particles and realize higher dispersion. This method involves the synthesis of colloidal sols, in which nanoparticles are stabilized in solution by the adhesion of specific surfactant or ligand molecules. [88] However, removal of these stabilizing molecules is still problematic. A key structural characteristic of LDHs is that the M²⁺ and M³⁺ cations are uniformly distributed within the layers without 'domains' of like cations. Therefore, introducing catalytically active metals into the layers of LDHs opens up new opportunities to generate high-performance supported metal/oxide catalysts. Calcination of the LDH precursors followed by reduction affords metal catalysts supported on MMOs and results in a strong interaction between the active metal and the concomitantly formed substrate, which prevents the aggregation/sintering of the nanoparticles during use and thus improves the stability of the active species. [21] Similarly, by taking advantage of the wide flexibility and ordered arrangement of the compensating anions in the interlayer galleries, intercalation of catalytically active species in the interlayer galleries of LDHs has been shown to be another effective way to obtain novel supported catalysts with improved dispersion and stability. The extent of the dispersion of the active sites can be controlled by modulation of the layer charge density (which depends on the ratio of M²⁺ to M³⁺ cations). [21]

### 2.2.1 Supported catalysts with active species derived from LDH layers

### 2.2.1.1 Monometallic catalysts derived from LDH layers

Transition metals with similar ionic radii to those of Mg²⁺ and Al³⁺ can be introduced into the layers of LDHs. [89] Therefore, a great number of supported metallic catalysts have been prepared by means of this LDH precursor approach. Takehira et al. [90] prepared a ternary NiCaAl-LDH as a precursor to obtain supported Ni catalysts for the partial oxidation of methane to synthesis gas. The

influence of the preparation method on the catalytic performance was also studied. Compared with the catalyst prepared by the impregnation method, the Ni catalyst derived from the LDH precursor exhibited both higher activity and selectivity to synthesis gas production, as well as less extensive coke formation. This excellent performance was ascribed to the use of an LDH containing homogeneously distributed $Ni^{2+}$ cations as a precursor to obtain stable and highly dispersed Ni metal particles on the surface of the support as well as the basic properties of the CaAl-MMO. Tichit and coworkers[91] employed a facile single-source precursor route to achieve green, well dispersed supported Ni-based materials using a NiMgAl-LDH precursor and studied their catalytic activity for the liquid-phase hydrogenation of adiponitrile. By taking advantage of the wide tunability of the metallic cations in the layers of LDHs, the effect of different Ni/Mg ratios on the catalytic performance was also investigated. The highest selectivity and yield (66% selectivity at 70% conversion, 50% yield at 85% conversion) in the half-hydrogenation of adiponitrile to aminocapronitrile was achieved using a catalyst with Mg/(Mg+Ni) = 0.20. IR spectroscopy of the material after treatment with CO showed that the catalyst with Mg/(Mg+Ni) = 0.20 possessed smaller $Ni^0$ ensembles and larger back-donation from $Ni^0$ sites to the $2\pi^*$ orbitals of CO associated with higher electron density at the Ni sites, which facilitated the desorption of aminocapronitrile and therefore improved the selectivity.

The acid-base character of MMOs can be controlled by changing the calcination conditions. Since it has been reported that the acid-base characteristics of a catalyst support have an influence on the hydrogenation reaction, therefore, the effect of varying the calcination and reduction temperatures on the catalytic performance of Ni/Mg(Al)O catalysts was investigated in the gas-phase hydrogenation of acetonitrile[92, 93] and valeronitrile.[94] The nature of the thermal treatment was found to strongly influence the surface acid-base character of the support and the lowest ratio of weak Brønsted acid sites to basic sites was obtained for the catalyst prepared by calcination at 623 K and reduction at 723 K. The Ni/Mg(Al)O catalyst activated under the above conditions exhibited the highest selectivity to monoethylamine (MEA), 94.6% at 47% acetonitrile conversion and it remained as high as 92% at almost full conversion (99%). Subsequently, the effect of adding other metal oxides was assessed.[95] Chen et al.[95] prepared highly-dispersed, Fe oxide-modified Ni catalysts derived from a quaternary NiMgAlFe-LDH precursor for partial oxidation of n-butanol for hydrogen production. It was found that the Ni-Fe oxide/MMO catalyst showed higher activity for hydrogen production compared to the Ni/MMO catalyst obtained from a NiMgAl-LDH precursor. BET and HRTEM results indicated that Ni-Fe oxide/MMO catalyst had a higher surface area (178.2 $m^2$/g) and a smaller mean particle size (5.6 nm), suggesting that a higher degree of dispersion of active metals led to enhanced catalytic activity. Furthermore, the $H_2$ yield of the Ni-Fe oxide/MMO catalyst remained stable near 4.03 mol-$H_2$/mol-butanol over a long-term (31 h) test. The high catalyst stability was ascribed to the enhanced thermal stability of LDH after the introduction of Fe, which resulted in 27.0% of the $Ni^0$ remaining unchanged even in the oxidative atmosphere of catalytic partial oxidation.

As well as metallic Ni, Cu and Ru are also very efficient active components of catalysts for hydrogenation and oxidation. Recently, Li et al.[96] prepared a quaternary CuZnAlZr-LDH as a precursor to supported Cu-based catalysts for $CO_2$ hydrogenation to methanol. The properties of the new catalysts were compared with those prepared using rosasite as a conventional precursor. The effect of varying the $Cu^{2+}/Zn^{2+}$ atomic ratio on the catalytic performance of the Cu/ZnAlZr-LDH-derived catalysts was also investigated. The

$Cu^{2+}/Zn^{2+}$ atomic ratio was found to significantly influence the dispersion of Cu. With increasing Cu content, the dispersion of Cu gradually decreased, while the exposed surface area of copper reached a maximum for a $Cu^{2+}/Zn^{2+}$ ratio of 2. Therefore, the highest catalytic activity and selectivity were obtained over the Cu/ZnAlZr-MMO catalyst with $Cu^{2+}/Zn^{2+}$ ratio of 2. Moreover, the structure of the precursor also had an influence on the catalytic activity. Compared to the catalysts derived from the rosasite precursor, the Cu/ZnAlZr-MMO catalyst possessed much higher specific surface area which facilitated the exposure of copper and thereby improved the activity. Supported Ru catalysts derived from a Ru/MgAl-LDH precursor were tested in the catalytic partial oxidation of $CH_4$ to produce syngas by Benito and coworkers.[97] A catalyst containing 0.25 wt.% Ru obtained from the LDH exhibited higher activity and stability than one prepared by an impregnation method, due to an enhanced interaction between the metal and MMO support, high carbon resistance and thermal stability. In addition, the effect of varying the Ru content on the performance of catalyst was also studied. As the Ru loading increased both the Ru dispersion and the interaction with the support decreased, leading to a decrease in activity.

As discussed above, powdered LDHs prepared by homogeneous precipitation are not ideal for large-scale practical applications. Al-containing LDHs can be synthesized *in situ* on the surface of $Al_2O_3$ spheres, which act as both the support and the sole source of $Al^{3+}$ cations. In this case, the adhesion between the LDH and the substrate is much stronger compared with materials obtained using the deposition method, owing to the presence of chemical bonds between the two phases, which increases the catalyst stability. Furthermore, the directed orientation of the LDH platelets with respect to the catalytically active component increases the accessibility and stability of the active sites and therefore enhances the catalytic activity. For example, Li et al.[19] reported the *in situ* growth of NiAl-LDH microcrystallites on a spherical $Al_2O_3$ support by means of surface activation using urea as the precipitant. After subsequent reduction in $H_2$, the resulting Ni/$Al_2O_3$ catalyst was used for the hydrodechlorination (HDC) of chlorobenzene (CB). Compared with the Ni/$Al_2O_3$ catalyst from a conventionally impregnated Ni($NO_3$)$_2$/$Al_2O_3$ precursor, the catalyst derived from the LDH/$Al_2O_3$ precursor showed a higher activity, due to larger surface area and higher metal dispersion, which resulted from the directed orientation of well-developed 2D platelet-like LDHs on the surface of alumina, as well as the uniform distribution of $Ni^{2+}$ in the LDH layers. Moreover, the formation of additional $AlO_4$ octahedra via Al-O-Ni linkages to the composite structure stabilized the active components and therefore enhanced the stability. The conversion remained over 95% at 370 °C after 16 h on stream. Similarly, Zhang et al.[98] also synthesized a Ni/$Al_2O_3$ catalyst by *in situ* growth of NiAl-LDH on the outer surface of the egg-shell γ-$Al_2O_3$ support using aqueous ammonia as the precipitant for selective hydrogenation of pyrolysis gasoline (PyGas). The resulted catalyst also exhibited preferable activity and stability. Recently, a magnetic core-shell structure $Fe_2O_3$@Cu/MgAl-MMO material was fabricated using a CuMgAl-LDH precursor and used as a catalyst for hydrogenolysis of glycerol reaction.[99] The inclusion of the magnetic $Fe_2O_3$ component facilitates the separation and recycling of the catalyst.

**2.2.1.2 Monometallic catalysts derived from LDH/C precursors**

Carbon materials such as graphene (G)[100], carbon nanotubes (CNT)[44,101,102] and carbonized precursors[101] have attracted enormous attention as potential catalytic materials by virtue of their large specific surface area, remarkable electrical conductivity,

excellent structural flexibility, high chemical/thermal stability and low cost. In some hydrogenation catalysts, the carbon species can serve not only as an electron-rich substrate but also as a reducing agent which can reduce the active species *in situ*.[100, 101] Therefore, combining LDHs with carbon materials is a powerful method to synthesize efficient catalysts. Li et al. obtained Ni/C catalysts from hybrid NiAl-LDH/C nanocomposite precursors for use in the hydrodechlorination of chlorobenzene.[101] It was reported that the reducing ability of the carbon species enhanced the metal-support interactions through electron transfer, which thus gave rise to more spillover hydrogen species on the metal-support interface involved in the hydrogenation process. In addition, the directed orientation of LDHs on the surface of the carbon species as well as the uniform distribution of $Ni^{2+}$ in the LDH layers enhanced the metal dispersion of the catalyst. Compared with the Ni/C catalyst obtained using a conventional impregnation method, the catalyst prepared from the NiAl-LDH/C nanocomposites showed higher catalytic activity (99.3% conversion for the Ni/C catalyst with a Ni loading of 18.7 wt%. Similarly, Ni/CNT[102] and Ni/graphene[100] catalysts were derived from a NiAl-LDH/poly(acrylic) acid (PAA) functionalized CNT nanocomposite precursor (Fig. 8) and a NiAl-LDH/G (Fig. 9) precursor, respectively and employed for the selective hydrogenation of *o*-chloronitrobenzene and cinnamaldehyde (CALD). Both of the composite catalysts showed excellent activity and selectivity, which was attributed to their high chemical/thermal stability and the presence of an electronic interaction between the metal and the support.
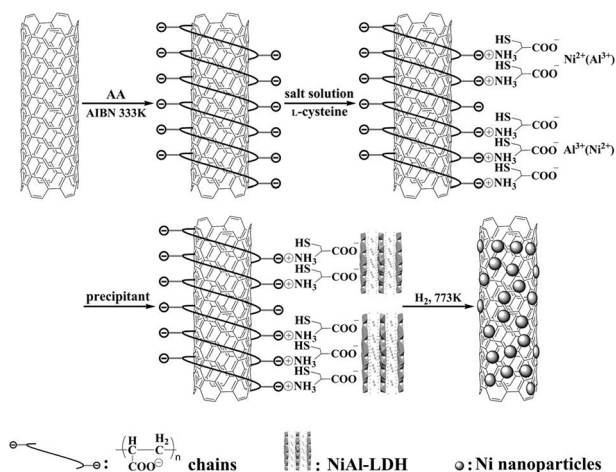


**Fig. 8** Schematic illustration of the synthesis of Ni NPs highly dispersed on CNTs (AA: acrylic acid; AIBN: 2,2-azobisisobutyronitrile). Reproduced from ref. 102. Copyright 2013 The Royal Society of Chemistry.
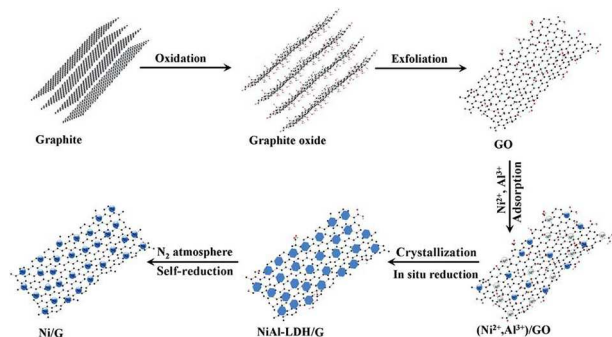


**Fig. 9** Schematic illustration of synthesis of a Ni/G nanocatalyst. The route consists of five steps: (1) oxidation of graphite to graphite oxide with a swollen interlayer distance; (2) exfoliation of graphite oxide via sonication to form a graphene oxide (GO) dispersion; (3) adsorption of metal ions onto the surface of GO via surface electrostatic interaction; (4) *in situ* nucleation and growth of NiAl-LDH nanoplatelets, simultaneously accompanied by the reduction of GO to graphene without any additional reducing agents; and (5) *in situ* autoreduction of NiAl-LDH/G to form the highly dispersed Ni/G nanocatalyst. Reproduced from ref. 100. Copyright 2013 The Royal Society of Chemistry.

Recently, Li et al.[103] fabricated a Ni–ZnO/C nanocatalyst by *in situ* reduction of hybrid NiAl-LDH/C precursor for selective hydrogenation of citral. Compared with the Ni/C catalyst, higher selectivity toward citronellol (>92%) was achieved over Ni–ZnO/C catalyst due to the modification of ZnO species as Lewis acid sites which simultaneously facilitated the activation of C=O bond. Hou et al.[44] assembled a multiwalled carbon nanotube (MWCNT)-pillared layered Cu/MgAlO MMO material for use as a catalyst for the hydrogenolysis of glycerol. The narrow pore channels generated by the ordered accumulation of MgAlO lamellae, the high surface area and the close contact between Cu/MgAlO and MWCNT enhanced the reducibility of CuO and facilitated hydrogen spillover, therefore resulting in excellent catalytic performance. Very recently, Feng et al.[104] fabricated a NiAl-LDH/reduced graphene oxide (RGO) composite support via depositing NiAl-LDH on the surface of GO. In this process, GO was partially reduced to RGO with certain topological defects and carbon vacancies. After loading Au NPs, the Au/NiAl-LDH/RGO hybrid catalyst was used in the oxidation of benzyl alcohol. The TON of the Au/NiAl-LDH/RGO catalyst reached 17893.4 after 10 h reaction, much higher than that of Au/RGO (2724.6) and Au/NiAl-LDH catalyst (12024.9). This preferable activity was mainly attributed to the defect sites and oxygenic functional groups which were considerd as anchoring centers for the nucleation and dispersion of the Au NPs and led to a smaller Au particle size in the NiAl-LDH/RGO composite support.,

### 2.2.1.3 Bimetallic catalysts

In recent years, bimetallic catalysts have received considerable attention. Such hybrid materials may offer opportunities for synergistic intermetallic interactions that lead to improvement in catalytic performance when compared to those of their pure constituent metals.[105-108] The wide flexibility of LDH composition makes a large number of elemental combinations accessible, which provides the opportunity to prepare LDH precursors for a wide variety of bimetallic catalyst systems.[109] There are two approaches generally used to prepare bimetallic catalysts based on LDH materials. The most widely used one is simultaneously introducing two active metals into the layers of LDHs followed by calcination and reduction processes. For example, Behrens et al.[110] developed a facile methodology for the preparation of highly dispersed intermetallic PdGa and PdZn catalysts using an LDH precursor-based approach. LDHs with different elemental combinations facilitated the formation of intermetallic compounds (IMCs). The catalytic performance of these IMCs was investigated in the hydrogenation of $CO_2$ and methanol steam reforming. It was found that the inclusion of Ga or Zn improved both the activity and selectivity in comparison with the monometallic Pd catalyst, since the introduction of Ga or Zn into the layers of LDHs led to a homogeneous distribution of Pd and an intimate interaction between PdGa or PdZn alloys and the support. As another example of IMCs, a highly dispersed Ni-In IMCs catalyst was derived from a NiMgIn-LDH precursor and demonstrated excellent catalytic activity and selectivity in the hydrogenation of α,β-unsaturated

aldehydes (Fig. 10).[111] The high activity was ascribed to the formation of highly dispersed Ni-In IMC NPs due to the atom-level interspersion of the active components in the layers of the LDH precursor.
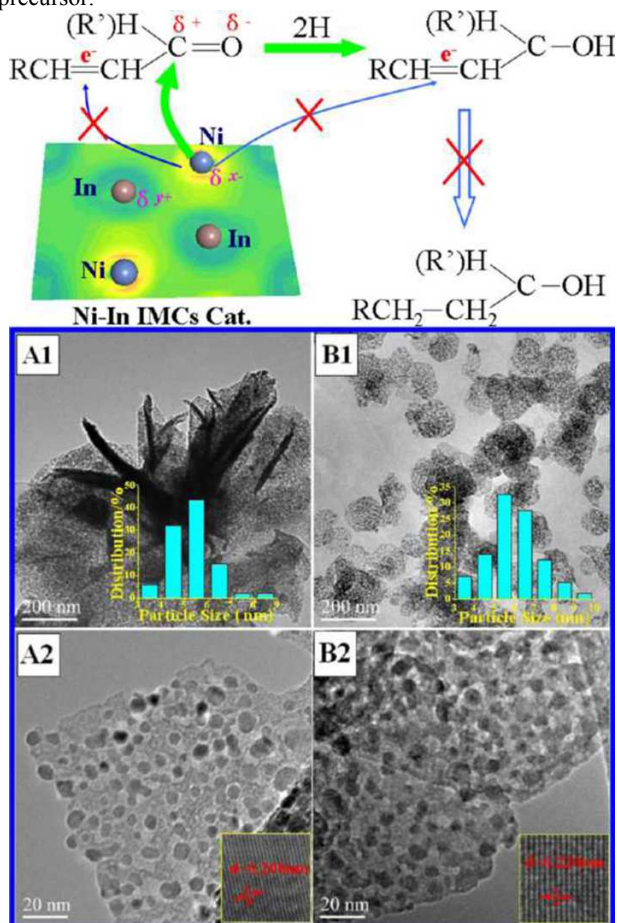


**Fig. 10** Schematic illustration of the reaction path for the selective hydrogenation of unsaturated carbonyl compounds over Ni-In IMC catalysts and TEM images of supported Ni-In IMCs: (A1) low- and (A2) high-magnification images for $Ni_2In/Al_2O_3$ and (B1) low- and (B2) high-magnification image for $Ni_2In_{3/7}MgO$. The insets show the size distribution (panels A1 and B1) and the HRTEM lattice fringes (panels A2 and B2) for the $Ni_2In$ and $Ni_2In_3$ NPs. Reproduced from ref. 111. Copyright 2013 American Chemical Society.

By taking advantage of the tunable composition of LDH precursors, a supported Ni-Ga IMCs catalyst [112] was synthesized by *in situ* reduction of an LDH precursor. Excellent catalytic behavior in semi hydrogenation of phenylacetylene was obtained over the Ni-Ga IMC catalyst with a styrene yield of 87.7%, which was much higher than that over most of the Ni catalysts previously reported in the literature. The remarkable increase in yield was mainly attributed to the enhancement of selectivity caused by the electron transfer from Ga to Ni and isolation of the active Ni sites by Ga in Ni-Ga IMCs; this was confirmed by XAFS measurements and density functional theory (DFT) calculations.

Subsequently, the preparation of NiCo bimetallic catalysts derived from NiCoMgAl-LDH precursors and their catalytic performance in the hydrogenation of acetonitrile was reported by Tichit and coworkers.[113] The catalyst obtained from a CoNiMgAl-LDH precursor calcined at 393 K and reduced at 893 K exhibited the highest selectivity to ethylamine (98.2% at 10% CH₃CN conversion). This high selectivity was attributed to the presence of Co inhibiting the undesired consecutive transamination reaction

which can occur between "imine-like" and "amine-like" species on both the metal and acid sites and on the metal sites alone. Zhang et al.[114] also prepared a NiCo catalyst by the same method for use in the selective hydrogenation of pyrolysis gasoline. Compared with a Ni catalyst prepared by the impregnation method, the bimetallic NiCo catalyst exhibited better catalytic performance since the introduction of appropriate amounts Co into the catalyst diluted the Ni phase, giving small ensembles prone to the formation of linear coordinated species as well as decreased surface acidity, which improved the catalytic activity. Additionally, it was proposed that the enhanced reducibility and smaller particle size of the NiCo bimetallic catalysts, as well as the relatively stronger interaction between Ni (or Co) species and the $Al_2O_3$ support, could suppress coke formation during the hydrogenation reaction and improve the stability. Analogously, Dragoi and colleagues[115] reported the preparation of a bimetallic NiCu catalyst by the direct reduction of a NiCuMgAl-LDH precursor. The catalyst exhibited significantly better activity in the hydrogenation of cinnamaldehyde in comparison with a monometallic Cu catalyst. Furthermore, the effect of varying the treatment temperature on catalytic performance was investigated. Interestingly, a Cu catalyst reduced at 150 ºC exhibited the same catalytic activity as a Ni catalyst reduced at 500 ºC. It was thus concluded that reducing such LDH precursors at low temperature offers a simple route to obtain highly dispersed and stable metallic nanoparticles, while also avoiding the time- and energy-consuming calcination step.

### 2.2.1.4 Supported oxide catalysts

In addition to acting as supports for metal catalysts, LDHs can also be used as precursors to generate a variety of MMO catalysts by controlled thermal decomposition. The topotactic nature of the LDH decomposition to metal oxides affords materials with a large specific surface area (100-300 $m^2g^{-1}$), a homogeneous and thermally stable dispersion of the metal ion components, synergistic effects between the elements and abundant acid and basic sites associated with the presence of $O^{2-}-M^{n+}$ acid-base pairs. [21]

For example, Ce-containing MMO catalysts were prepared by the calcination of a CeMgAl-LDH precursor and used for the complete oxidation of methane. Calcination afforded a mixture of inert MgO and $Al_2O_3$ phases which could be considered to act as a support to stabilize and disperse the active transition metal oxide. The Ce mixed oxide catalysts showed higher conversion and stability compared to other transition metal (Sm, Dy and Yb) mixed oxides, due to the different reducibility of transition metal.[116] Furthermore, the authors also claimed that the presence of a $Ce^{4+}/Ce^{3+}$ redox couple facilitates adsorption of oxygen species on the catalyst surface, which also enhanced the catalytic activity. In addition, the influence of varying the cerium content (5-20 wt.%, as well as pure $CeO_2$ for comparison) on the catalytic activity was studied. The activity of the $Ce_xMgAl$-MMO catalysts increased with increasing Ce content up to 10%. The $Ce_xMgAl$-MMO catalyst with 20 wt.% Ce showed a marked decrease in activity, probably attributed to the significant decrease of the specific surface area caused by an excess of ceria and pure $CeO_2$ was an even less active catalyst. Marcu et al.[117] investigated the use of MMgAl-MMO catalysts (M = Mn, Fe, Co, Ni, Ag and Pd) prepared via an LDH precursor route for the complete oxidation of methane and other short-chain hydrocarbons. The noble metal-containing PdMgAl-MMO catalysts proved to be the most active, but the least stable, catalysts. Among the non-noble metal-containing catalysts, the CuMgAl-MMO catalyst showed the highest activity with total conversion being reached at 858 K and also the highest stability, indicating that the presence of highly

reducible metal oxide species played an important role in the high catalytic performance.

Additionally, CuCo-based MMO catalysts synthesized from a uniform $Cu_xCo_{3-x}Al$-LDH precursor were employed for the complete oxidation of benzene.[118] The Cu/Co ratio was found to have an impact on the specific surface area and pore size of the catalyst, as well as the reducibility of $Cu^{2+}$ species. $Cu_{0.5}Co_{2.5}Al$-MMO showed the maximum activity of 2.41 mmol $g^{-1}_{cat}h^{-1}$, with 90% benzene conversion at 290 °C at a high space velocity (SV = 60,000 mLg$^{-1}$h$^{-1}$), which was significantly higher than that obtained with the $Cu_3AlMMO$ catalyst (0.27 mmol $g^{-1}_{cat}h^{-1}$ with 8% conversion). $Cu_{0.5}Co_{2.5}Al$-MMO also showed high stability over extended time on benzene stream and resistance to water vapor due to the strong interaction between the active oxide and the inert $Al_2O_3$ which effectively prevented the migration and aggregation of the active component. Recently, Li et al.[119] reported a heterogeneous Co-based catalyst by *in situ* growth of CoZnAl-LDH precursor on amorphous alumina microspheres followed by calcination for solvent free oxidation of ethylbenzene. The obtained CoZnAl-MMO/$Al_2O_3$ catalyst showed high dispersion of Co species due to well-developed 3D flower-like CoZnAl-MMO platelets as well as the separating effect of the resulting ZnO phase and therefore exhibited much higher catalytic activity, selectivity and stability compared with the catalyst prepared by impregnation method. Catalytic hydrogenation of cinnamaldehyde (CNA)[120] was also investigated over Cu oxide materials obtained by calcination of a CuMgAl-LDH precursor. The strong base sites at the surface and the strong interaction between active material and inert support resulted in a high dispersion of copper with reasonable particle homogeneity leading to high catalytic activity. The presence of magnesium noticeably enhanced the selectivity of the Cu-based catalysts with respect to the hydrogenation of the carbonyl group rather than the hydrogenation of the C=C bond in CNA. In addition, taking advantage of the flexibility in LDH composition, NiMgAl, NiCoMgAl and CuZnAl MMO materials were also prepared from the corresponding LDH precursors and used as catalysts for the selective hydrogenolysis of glycerol.[121] The CuZnAl MMO exhibited the best catalytic performance with 93-94% selectivity toward propylene glycol at a glycerol conversion of 52%; this was attributed to it for having stronger surface acid-base properties, smaller crystallite size and higher surface area than the other MMO catalysts.

### 2.2.2 Supported catalysts with active species derived from guests in the LDH interlayer galleries

Although exploiting LDHs containing active metallic cations in the layers has been reported to be a successful way to prepare precursors to highly efficient supported catalysts, this approach is not always possible owing to the inability of some active metal cations to be incorporated into the layers. In this case, materials with anionic complexes of the target metal cation can be intercalated into interlayer galleries between the positively charged brucite-layers and subsequently converted to highly dispersed metal catalysts. The intercalation of catalytically active species in the interlayer galleries of LDHs followed by reduction at specific temperatures has been shown to be capable of improving catalytic stability and recyclability when compared with the corresponding homogeneous catalyst.[122] Tichit and coworkers[123] fabricated a Ni-based catalyst by immobilization of negatively charged Ni colloidal suspensions into the interlayer galleries of MgAl-LDH followed by calcination and reduction at high temperature. Sintering of the particles during reduction process was inhibited by the interaction between the active metal and the MMO support derived from the

LDH precursor and therefore the catalyst exhibited excellent catalytic properties for methane reforming. Wei et al.[124] investigated the effect of intercalated anions on the dispersion of an active metal component obtained from the layers of LDH precursors. For example, when $MoO_4^{2-}$ anions were intercalated into a FeMgAl-LDH, subsequent calcination and reduction afforded an extremely high density of small (3-20 nm) Fe NPs having a narrow size distribution and high stability. It was suggested that Fe NPs were embedded in the MMO flake due to a pinning effect of Mo around the Fe NPs. The presence of strong interactions between Fe NPs and the support effectively prevented sintering, leading to high stability. Recently, Li et al.[125] prepared a supported $MnO_2$ catalyst by intercalating small amount of $MnO_4^-$ anions into MgAl-LDHs followed by reduction at high temperature. The catalyst exhibited better stability and reusability in the solvent-free aerobic oxidation of ethylbenzene than a previously reported $MnO_2/\alpha$-$Al_2O_3$ catalyst prepared by the impregnation method. This was interpreted in terms of a confinement effect of the LDH which suppressed the migration and aggregation of $MnO_2$. Furthermore, calcination of a CuZnAl-LDH precursor intercalated with $[Ce(dipicolinato)_3]^{3-}$ anions prepared by an anion exchange method (Fig. 11) was shown to afford Cu-Ce-O MMOs which were active catalysts for the oxidation of phenol.[126] The authors showed that the introduction of Ce significantly promoted the catalytic activity due to the interaction between Cu and Ce centers, which had a significant effect on the specific surface area, pore structure and chemical state of Cu and Ce in the resulting Cu-Ce-O MMOs.
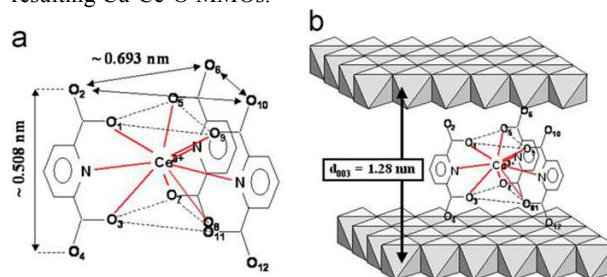


**Fig. 11** Representation of the suggested interlayer arrangement of $[Ce(dipicolinato)_3]^{3-}$ anions in interlayer galleries of LDH. Reproduced with permission from ref.126. Copyright 2011 Elsevier.

Similarly, supported CuO catalysts for use in methane total oxidation had been obtained by intercalation of Cu-containing anionic complexes into a ZnAl-LDH host followed by calcination.[127] By virtue of ability to tune the anions in the interlayer galleries of LDHs, the effect of varying the Cu content on the catalytic performance was also investigated by controlling the amount of intercalated Cu complex. $Cu_{10}ZnAl$-MMO (10% Cu) mixed oxide catalysts showed the highest activity and stability as a result of the optimum dispersion of the CuO active species and the strong interaction between CuO particles and the support. Li et al.[128] synthesized a series of hybrid LDH-C composites supported Pd nanocatalysts via a facile one-step hybridization-reduction route, which involved the assembly of composites of $PdCl_4^{2-}$-intercalated MgAl-LDH and amorphous carbon through the carbonization of glucose and simultaneous reduction of Pd(II) species, without further chemical modification of the supports. The as-formed supported Pd nanocatalysts were found to be more active and selective in the liquid-phase hydrogenation of citral to citronellal compared with the traditional activated carbon supported Pd catalyst due to uniform Pd NPs with small diameter, as well as the strong metal–support interaction. A high selectivity of citronellal (87.4%) at a conversion of 100% was achieved over the as-formed

catalyst with the Pd loading of 2.7 wt%. Similarly, a carbon supported boron-promoted Ni catalysts (B–Ni) via an *in situ* self-reduction process of borate-intercalated NiAl-LDH/C was also reported.[129] The resulting spherical B-modified Ni NPs were homogeneously dispersed and anchored tightly on the surface of the support. A suitable amount of boron was found to be essential for not only the enhanced Ni dispersion but also pronounced surface Ni–B interaction, as well as strong Ni–B–support interactions, accounting for significantly enhanced activity in hydrodechlorination of chlorobenzene, in comparison with a B-free Ni catalyst.

In recent years, co-intercalation of two types of anionic species has also attracted much attention, because the adjustable height of the 2D interlayer galleries in LDHs can provide great opportunities for a significant enhancement of catalytic performance.[116] Using the successive anionic exchange method, MgAl-LDH has been intercalated with negatively charged copper hydroxy citrate colloids and then hexachloroplatinate species.[130] The intercalated LDHs was then used as the precursor of a bimetallic PtCu catalyst for the hydrogenation of nitrate anions. Compared with the best catalyst prepared by the impregnation route described previously in the literature, the anionic exchange route afforded a higher dispersion of platinum and copper nanoparticles in the reduced catalysts leading to much improved catalytic performance, with a nitrate conversion of 52% and nitrogen selectivity of 36%.

# 3. Some promising application prospects of supported catalysts based on LDHs

Oxidation and hydrogenation are key processes in many areas of the chemical industry, including petrochemicals, fine chemicals, clean energy, environmental protection and biomass utlization. In this section, some representative reactions from these fields are chosen to explore the application possibilities of LDH-based catalysts with a focus on the structure-performance relationships in a featured reaction.

## 3.1 Semi-hydrogenation of acetylene

Ethene is an important polymerization feedstock and intermediate in many industrial reactions. It is usually produced by thermal or catalytic cracking of higher hydrocarbons, during which a minute amount of acetylene is inevitably produced. As the traces of acetylene are detrimental to the subsequent polymerization, removal of acetylene in an excess of ethene is essential.[131-133] There are two general approaches to reduce the acetylene concentration in the feedstock—separation and selective hydrogenation. In principle, the latter is the more attractive method because of its relative simplicity and low cost, but requires the development of highly selective hydrogenation catalysts.[134,135]

The reaction scheme in Fig. 12 shows the partial hydrogenation of acetylene and the main undesirable side reactions, namely over-hydrogenation and the formation of green oil.[136] The hydrogenation of ethene to ethane results in a loss of ethene for the subsequent polymerization, while the deposition of high molecular weight oligomeric species on the catalyst leads to a decrease in overall activity and ethene selectivity as well as loss of hydrocarbon.[136-138] Supported palladium based catalysts are commonly used as the catalyst for selective hydrogenation of acetylene. In terms of thermodynamics, the selective hydrogenation of acetylene in a rich ethene stream is a feasible process because the adsorption energy of ethene on Pd atop sites is much lower than that of acetylene.[139] In the absence of acetylene, ethene is hydrogenated readily on Pd. In the industrial production, CO is employed as an additive to poison

some of the active sites in order to decrease the formation of ethane and oligomers.[140] However, in order to make the process more eco-friendly and economical, developing highly selective catalysts in the absence of CO has become a great challenge.
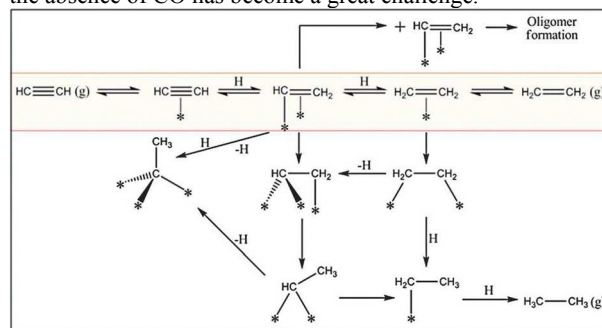


**Fig.12** Schematic representation of the catalytic cycle for hydrogenation on a palladium-based catalyst. The path on the pink background is the only one that a good co-catalyst or promoter should perform. Reproduced with permission from ref. 136. Copyright 2012 The Royal Society of Chemistry.

Several approaches have been utilized to improve ethene selectivity at high acetylene conversion, including the addition of a second metal, choice of a suitable support and strengthening of the metal-support interaction.[141-143] LDHs have been widely studied as supports for catalysts for the partial hydrogenation of acetylene. Recently, Li and coworkers[144] synthesized NiTi-LDH with an abundance of defect sites by the hydrothermal method and used it as the support for the preparation of a PdAg nanoalloy catalyst. Due to abundance of defect sites on the surface of the LDH support, PdAg alloy particles with a small size were dispersed homogeneously on the surface of NiTi-LDH. Furthermore, the interface between the $Ti^{3+}$ species and the active metals was shown to be a new active site which further enhanced the activation and dissociation of hydrogen contributing to the enhanced catalytic activity of the PdAg/NiTi-LDH catalyst compared with PdAg catalysts supported on $TiO_2$ or $Ni(OH)_2$. In addition to the enhanced activity, higher selectivity towards ethene was also observed over the PdAg/NiTi-LDH catalyst. This was attributed to the electron transfer from the $Ti^{3+}$ species to Pd which resulted in an increase in electron density and the linearly coordinated sites of Pd and thereby facilitated the desorption of ethene. Even when the conversion of acetylene reached 90%, ethene selectivity over the PdAg/NiTi-LDH catalyst remained as high as 82%, some 30% higher than that obtained using the commercial alumina supported catalyst. Subsequently, a strong metal-support interaction (SMSI) effect was obtained by reducing the PdAg/NiTi-LDH catalyst, whereby the Pd atoms accepted electrons donated by the $Ti^{3+}$ species leading to a further increase in selectivity. Moreover, this reduced catalyst also demonstrated superior stability. One of the reasons for this was the enhanced resistance against carbon deposition leading to less blocking of the active sites; the other was the excellent structural stability of the PdAg nanoalloys which was ascribed to the presence of the strong interaction between the PdAg nanoalloys and the support.

Li and coworkers also employed a MgAl-LDH as a support to prepare Pd catalysts with specific morphology and uniform dispersion by a one-step precipitation-reduction method and investigated the relationship between morphology of the active metal and the catalytic performance.[74] Compared with the LDH-supported truncated octahedral Pd particles enclosed by (111) and (100) facets, the tetrahedral particles surrounded by only (111) facets exhibited higher ethene selectivity, suggesting that the Pd(111) facet was the preferred facet in the selective hydrogenation

of acetylene to ethene. They further took advantage of the excellent adsorption properties of LDHs to synthesize a MgAl-LDH-supported Pd nanowire catalyst[75] and a bimetallic PdAu three-dimensional nanoflower catalyst[145] by the immobilization method and explored the influence of defect sites on the catalytic performance. The results indicated that the defect sites at crystal boundaries of Pd nanowires were more active owing to the exposure of larger amounts of Pd atoms, the higher Pd dispersion and the enhanced capacity for $H_2$ activation/dissociation. At 80% acetylene conversion, the selectivity of the LDH-supported Pd nanowire catalyst was 69%, much higher than the values reported in the literature for Pd/SiO$_2$ (20%), Pd-Ti/SiO$_2$ (37.5%) and Pd/Zn-modified Al$_2$O$_3$ (64%) at the same conversion. Compared with previously reported small particle PdAu catalysts, the supported PdAu nanoflower-like catalyst showed not only higher activity and selectivity but also much better stability, owing to its complex morphology, abundance of defect sites and synergetic effects caused by the interactions between the components units. Behrens and coworkers[146] synthesized an intermetallic Pd$_2$Ga catalyst using the LDH precursor synthesis approach. The resulting Pd$_2$Ga/MgO/MgGa$_2$O$_4$ material exhibited a large specific surface area (100-120 m$^2$g$^{-1}$) and strong interaction between Pd$_2$Ga NPs and the MgO/MgGa$_2$O$_4$ support, accounting for its excellent activity and high selectivity.

As mentioned previously, hybridization of LDHs with other materials to afford hierarchically structured catalysts can lead to enhanced performance as a consequence of the synergy between two materials as well as the tailored morphology. In 2009, Li and co-workers[19] combined NiAl-LDH with spherical alumina—which was the most widely used industrial support by virtue of its regular shape, microporosity, excellent physical strength and mass transfer—to obtain a hierarchically structured Ni catalyst. Subsequently, they synthesized Pd/MgAl-LDH *in situ* on the surface of spherical Al$_2$O$_3$ using hexamine as both the precipitant for LDH and the reductant for Pd$^{2+}$.[76] Interestingly, most of the Pd NPs were plate-like triangular or tetrahedral in shape and dispersed homogeneously on the surface of MgAl-LDH/Al$_2$O$_3$, which was ascribed to a template effect of the LDH during the reduction of Pd$^{2+}$. Additionally, the oriented growth of LDH microcrystallites with regular size and well-developed two-dimensional platelet structure increased the specific surface area and decreased the surface acidic density of the Al$_2$O$_3$ support, which contributed to an enhancement of both activity and selectivity compared with the Pd/Al$_2$O$_3$ catalyst. After calcination, the catalyst was transformed into Pd/MgO-Al$_2$O$_3$ which exhibited high stability because of the suppression of carbonaceous deposition and the strong metal-support interactions. Importantly, these spherical catalysts with uniform size could be easily separated and recycled. Subsequently, Li and co-workers[109] developed a facile single-source precursor route to a well-dispersed bimetallic Pd-Ga/MgO-Al$_2$O$_3$ catalyst by *in situ* growth of an LDH on the surface of spherical γ-Al$_2$O$_3$. Ga$^{3+}$ was incorporated with a high degree of dispersion in the brucite-like layers of the LDH and PdCl$_4^{2-}$ anions were uniformly dispersed in the interlayer galleries of the LDH. Calcination of the LDH precursor afforded MgO and Al$_2$O$_3$ microcrystals which acted as a net to trap the Pd-Ga nanoalloy particles formed in the concomitant reduction process in fixed positions (Fig. 13). The resulting bimetallic Pd-Ga (1:5) catalysts exhibited comparable activity and much higher ethene selectivity (82% selectivity at 90% conversion) than the monometallic Pd catalyst (55% selectivity at 90% conversion). The significantly enhanced activity of the bimetallic catalyst was ascribed to the higher degree of dispersion of the Pd-Ga nanoalloy particles. The improved selectivity was attributed to the synergistic effects in the bimetallic Pd-Ga nanoalloys. On one

hand, electronic effects gave rise to a kinetic effect due to the decreased availability of hydrogen and a decrease in the chemisorption strengths of acetylene and ethene. On the other hand, a geometric effect—namely the isolation of the palladium active sites—led to weakly π-bonded acetylene on top of the isolated Pd atoms. More significantly, after continuous reaction for 48 h, the Pd-Ga (1:5) /MgO-Al$_2$O$_3$ catalyst still retained good catalytic performance due to the net trap confinement effect, which suppressed the migration and aggregation of the bimetallic Pd-Ga nanoalloy particles.
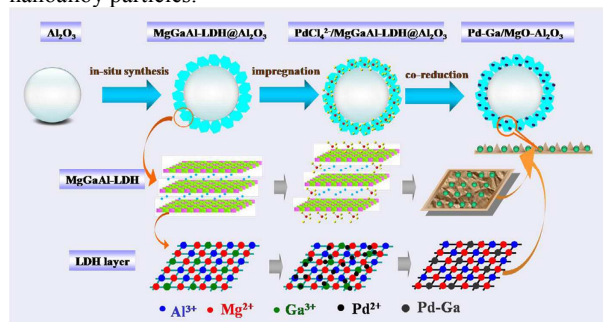


**Fig. 13** Synthesis of the supported bimetallic Pd-Ga catalysts derived from PdCl$_4^{2-}$/MgGaAl-LDH@Al$_2$O$_3$ precursor. Reproduced with permission from ref.109. Copyright 2014 Elsevier.

In conclusion, the catalysts prepared by the *in situ* growth of LDH precursors on the surface of alumina supports not only retain the regular shape, microporosity and excellent physical strength of the alumina support—which contributes to excellent mass transfer, good stability and easy recovery—but also possess improved metal dispersion and surface acid-base properties, leading to enhanced activity and selectivity. Compared to the corresponding powdered catalysts, hierarchically structured LDH@Al$_2$O$_3$ supported catalysts have much better prospects for practical application in the hydrogenation of acetylene.

### 3.2 Hydrogenation of dimethyl terephthalate

1, 4-cyclohexanedimethanol (CHDM) is widely used as a linker molecular in the polymer industry. It is, for example, preferred over ethene glycol as a building block in the production of polyester fibers for applications involving polycarbonates and polyurethanes.[147] In the current industrial process, CHDM is produced from dimethyl terephthalate (DMT) in two steps in two reactors. The first step is the highly exothermic conversion of DMT into dimethylcyclohexane-1,4-dicarboxylate (DMCD) at temperatures of 160-180 °C and H$_2$ pressures in the range 30-48 MPa. The intermediate DMCD is then converted into CHDM at about 200 °C with an H$_2$ pressure of about 4 MPa.

In the first step, although various supported metal catalysts such as Pd, Ru and Ni have been reported, only Pd can be employed in the industrial hydrogenation of DMT to DMCD because of its high catalytic activity and poisoning resistance. However, prevention of aggregation of the active phase at the high temperatures involved is a great challenge. To address this issue, Pd NPs supported on LDH-modified industrial θ-alumina spheres were prepared as a new catalyst for selective hydrogenation of DMT.[148] In this process, MgAl-LDHs were synthesized by decomposition of urea dissolved in an aqueous solution of Mg$^{2+}$ impregnated into θ-alumina. Introduction of the Pd precursor was also effected by impregnation. The formation of MgAl-LDH microcrystallites on θ-Al$_2$O$_3$ resulted in a tailored reticular morphology and increased surface area, leading to a uniform distribution of Pd NPs with a much smaller mean Pd particle size of about 4 nm compared with conventional

Pd/Al$_2$O$_3$ (12 nm) and Mg-modified Pd/Al$_2$O$_3$ (7 nm) catalysts. Importantly, the new catalyst exhibited excellent stability, retaining about 96.0% conversion of DMT, 98.5% selectivity for DMCD and a 95.0% yield of DMCD after a reaction time of 28 h. This was attributed to the Pd NPs being strongly immobilized on the modified support. Zhang et al.[149] extended this work by fabricating a series of MgAl-MMO-Al$_2$O$_3$ supported bimetallic PdRu catalysts. The RuPd/MMO-Al$_2$O$_3$ catalyst with total metal loading of 0.3 wt.% and Ru:Pd ratio of 1:1 exhibited much higher DMT conversion and DMCD yield than RuPd/Al$_2$O$_3$, while also giving high DMCD selectivity (~96.0%). They suggested that the LDH-modified support offers local confined spaces where the NPs were positioned, which could be responsible for the limited supply of accessible surface for hydrogen overspill towards the support surface. In addition, a larger number of acidic sites—especially ones with medium intensity—were present in the PdRu/LDH-Al$_2$O$_3$ catalyst and these could also contribute to the enhanced reactivity.

In the second step, CHDM is produced industrially by the catalytic hydrogenation of DMCD over CuCr-based catalysts. In spite of the high yield of the desired product, the toxicity of such types of Cr-containing catalysts, however, can cause quite serious environmental pollution, which thus limits the large-scale practical applications. Therefore, it is imperative to look for Cr-free highly efficient catalysts for the hydrogenation of DMCD. Li and coworkers[150] prepared a highly dispersed Cu/MgAl-MMO catalyst derived from a CuMgAl-LDH precursor. The resulting Cu-based catalysts afforded 100% conversion with 99.8% selectivity for times on stream of up to 200 hours. The synergy between the metallic copper species and surface Lewis basic sites coming from MgO support led to the formation of an intermediate with nucleophilic activity at the oxygen atom, thus improving the reactivity of the ester group in the DMCD molecule. The excellent stability was ascribed to the stabilizing effect of the MgO-Al$_2$O$_3$ phases in the catalyst, which prevented the aggregation of Cu NPs (Fig. 14). Subsequently, a Cu-based catalyst derived from CuZnAl-LDH precursor was also reported.[151] The introduction of Zn species further improved the dispersion of Cu species and long-term stability of the catalyst. Such low-cost and environmentally friendly Cr-free Cu-MMO catalysts are of great potential importance for the industrial production of CHDM.

To sum up, DMT hydrogenation using LDH-based catalysts has great potential in for application in CHDM production. The anchoring effect of LDHs prevents the aggregation of the active phase at high temperature in the first step and the synergy between metallic species and surface Lewis basic sites allows the materials to replace the toxic catalyst currently used in the second step. However, there is still abundant room to develop more highly performing LDH-based catalysts for the hydrogenation of DMT by using other LDHs.
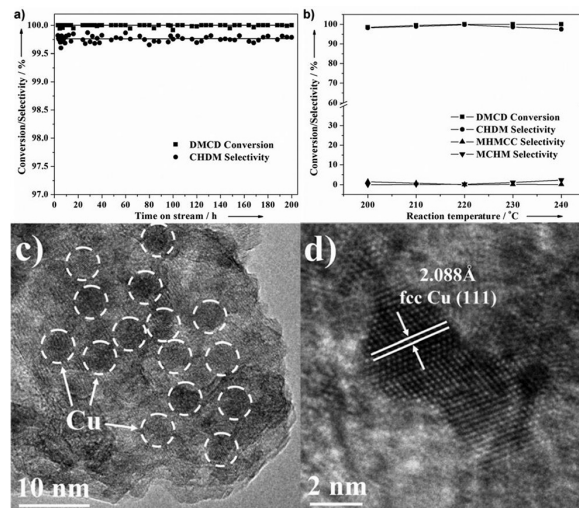


**Fig. 14** Hydrogenation performance of the Cu/Mg(Al)O catalyst as a function of time on a stream at 220 °C (a); DMCD conversion and product selectivities as a function of reaction temperature (b) over the Cu/Mg(Al)O catalyst; TEM (c) and HRTEM (d) images of Cu/Mg(Al)O catalyst. Reproduced with permission from ref.150. Copyright 2013 The Royal Society of Chemistry.

### 3.3 Methanation of CO/CO$_2$

Combustion of natural gas gives only CO$_2$ and H$_2$O without any other byproducts and is regarded as a more environmentally friendly energy resource than coal or oil. However, natural gas is a non-renewable resource and therefore the use of synthetic natural gas (SNG) as a substitute is attracting increasing attention. So far, several methods have been developed for the production of SNG, such as coal-to-SNG and methanation of CO/CO$_2$.[152,153] Methanation has become the most popular technology for the synthesis of SNG because, unlike other processes, it not only discharges no pollutants but also consumes a greenhouse gas as a reactant. The methanation reaction is also important in ammonia synthesis where it is employed to remove the final traces of CO/CO$_2$ from synthesis gas. A number of metal catalysts have been employed in methanation, such as Ni, Fe, Co, Ru and Rh. Ni-based catalysts have the advantage not only of low price, but also give high activity and selectivity. However, the prevention of rapid deactivation at high temperatures resulting from the exothermic reaction is the main challenge in the industrial application of Ni-based catalysts, since this leads to the sintering of Ni particles and facile carbon deposition.

LDHs have been widely employed in the synthesis of Ni-based catalysts with a high degree of dispersion and stability by utilization of anchoring effects to enhance the immobilization of the active phase. Gabrovska et al.[154,155] reported a Ni/Al$_2$O$_3$ catalyst prepared by reduction of a NiAl-LDH for methanation. The high dispersion of Ni decreased the reaction temperature to 260 °C. Furthermore, using positron annihilation spectroscopy, high-angle annular dark field scanning transmission electron microscopy (HAADF-STEM) and EXAFS, Wei and coworkers[152] found that abundant surface defects in nanocatalysts—such as Ni vacancy clusters and Ni monovacancies—which served as new active sites for the reaction were obtained in the *in situ* topotactic transformation of NiAl-LDH to Ni/Al$_2$O$_3$ (Fig. 15). Therefore, dramatically higher activity was obtained over the hierarchical flower-like Ni/Al$_2$O$_3$ catalyst derived from Al$_2$O$_3$@NiAl-LDH than that over a Ni catalyst prepared by a traditional impregnation method. When the conversion reached 50%, the reaction temperature was 74 °C lower than that required for the impregnated

catalyst. Moreover, after 252 h on stream, the decrease in $CO_2$ conversion was only 7% and the excellent stability was attributed to the strong metal-support interaction. Song et al.[156] exploited the compositional flexibility of LDHs by introducing Fe (III) into a NiAl-LDH and using the resulting ternary LDH as the precursor to a mesoporous bimetallic $NiFe/Al_2O_3$ catalyst. The introduction of Fe (III) into the LDH layers further decreased the particle size of Ni and thus enhanced the activity of the resulting catalysts, with the yield of methane reaching 58.2% at 220 °C.
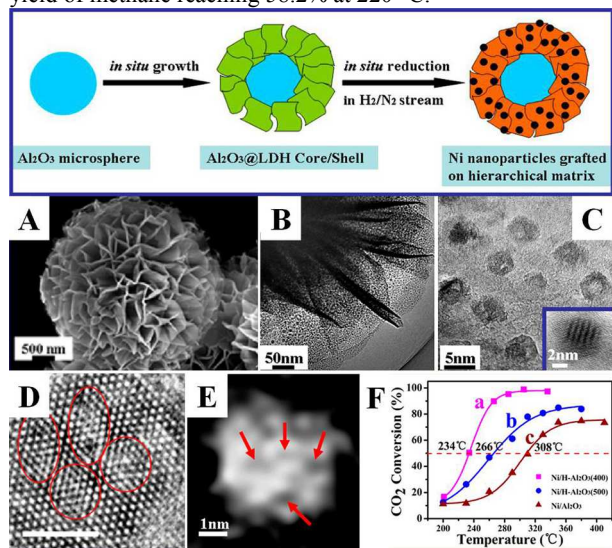


**Fig. 15** Illustration of the formation of Ni NPs with high dispersion and high density on a hierarchical flower-like $Al_2O_3$ matrix via an *in situ* reduction process of a $Ni_{II}Al_{III}$-LDH precursor; (A) (B) SEM images of the flower-like NiAl-LDH; (C) (D) HRTEM images of the flower-like NiAl-LDH; (E) High-angle annular dark field (HAADF) STEM images of Ni nanoparticles in the sample of flower-like NiAl-LDH; (F) Profiles of $CO_2$ conversion vs. temperature for $CO_2$ methanation in the presence of the flower-like NiAl-LDH. Reproduced with permission from ref. 152. Copyright 2013 American Chemical Society.

In summary, because of its properties such as the high dispersion of metallic cations in the layers and anchoring effect on metallic species during calcination and reduction steps, LDHs are potential materials for application in industrial methanation. However, there is still a need to synthesize multifunctional catalysts based on LDHs. For example, a number of studies have reported that basic catalysts are more resistant to carbon deposition.[157,158] Therefore, LDHs and MMOs as representative solid base materials are very attractive. Moreover, active metals such as Co and Ru can be incorporated into the LDH layers, which suggests a wide variety of highly stable dispersed catalysts with different active metals could be designed for use in methanation.

### 3.4 Epoxidation of olefins

Epoxides are commercially important intermediates for the synthesis of fine chemicals and pharmaceuticals such as ethene glycol, ethanolamines and detergents, because of their high chemical reactivity resulting from the three-membered ring.[159,160] They are traditionally produced by chlorohydrination of olefins followed by dehydrochlorination with a base, or by direct oxidation of olefin using oxidizing agents such as organic peracids, $H_2O_2$ or molecular oxygen.[161] In recent years, in the light of environmental protection and security issues, the method of direct olefin oxidation with molecular oxygen has gradually replaced other methods in industrial production. For the rational design and controllable synthesis of efficient catalysts for olefin epoxidation, it is necessary

to concentrate on the reaction mechanism. Recent DFT calculations, surface science experiments and kinetic isotope studies have suggested that the selectivity to epoxide was controlled by a reaction network of competing elementary pathways whereby a surface oxametallacycle (OMC) intermediate formed by the reaction of surface adsorbed atomic oxygen with an olefin undergoes isomerization reactions on the active phase to form the selective $(k_1)$ product—epoxide or aldehyde—which subsequently reacted to form more unselective $(k_2)$ combustion products, such as $CO_2$ and $H_2O$.[162-165] Therefore, the challenge in olefin epoxidation is to perform heterogeneous catalytic reactions leading to C-C or C-O bond formation.

It is generally considered that the presence of a base favors the construction of C-C and C-O bonds. Solid base catalysts are thus widely used in heterogeneous catalytic epoxidation of olefins. LDHs are a solid base, possessing an abundant array of hydroxyl groups on the layers. Moreover, the interlayer anion-exchange capability of LDH provides opportunity to firmly immobilize active anionic complexes in the interlayer galleries. Polyoxometalates (POM) are a large class of anionic species which can be used as catalysts for oxidation reactions such as epoxidation, due to their oxidative stability and high efficiency. Significantly, unlike most other supports, LDHs provide the possibility of protecting the epoxide formed against hydrolysis caused by the inherent acidity of POM.[166] In addition, the intercalation of POMs into the interlayer galleries of LDHs can inhibit deactivating dimerization or self-oxidation reactions, which leads to the high stability of LDH-POM catalysts.[167] In the 1990s, Jacobs and colleagues[159] reported that an NiAl-LDH exchanged with tungstate anions was an effective catalyst for oxidative bromination and bromide-assisted epoxidation by $H_2O_2$ (Fig. 16). In comparison with the homogeneous reaction using tungstate, nearly 200 times higher conversion was obtained over the LDH-based catalyst due to the spatial organization and electrical shielding. It was speculated that the large positive electric potential of the $WO_4^{2-}$-LDH surface induced an enrichment of bromide ions close to the surface. Furthermore, the simultaneous presence of bromide and peroxotungstate anions on the catalyst surface decreased the electrostatic repulsion between these negatively charged reaction partners. This kind of low cost, clean and efficient catalyst has thus attracted extensive attention.
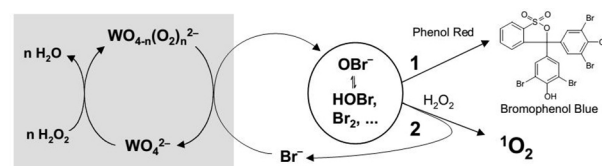


**Fig. 16** Catalytic cycle for bromination with LDH exchanged with tungstate. Reproduced with permission from ref. 159. Copyright 1999 Nature.

Subsequently, Li et al.[168] immobilized a series of POM anions such as $[WZn_3(ZnW_9O_{34})_2]^{12-}$ (ZnWO), $[WCo_3(CoW_9O_{34})_2]^{12-}$ (CoWO), $[WZnMn_2(ZnW_9O_{34})_2]^{12-}$ (MnZnWO) and $[PW_{11}O_{39}]^{7-}$ (PWO) into the interlayer galleries of MgAl-LDH by a selective ion-exchange method and used the products as catalysts for the epoxidation of allylic alcohols. Compared with the corresponding homogeneous Na-POM catalysts, the LDH-intercalated POM catalysts showed a significant enhancement in the selectivity for the epoxidation of various allylic alcohols under mild and organic solvent-free conditions which was attributed to the cooperative interaction between the POM guest and the LDH. For example, the MgAl-ZnWO catalyst showed up to 99% epoxide selectivity, 95% $H_2O_2$ efficiency and a TOF of 37200 $h^{-1}$ without the need for any

basic additives or pH control. The same group also immobilized ZnWO into the interlayer galleries of MgAl-LDH by a similar method.[169] Excellent activity (TOF up to 18,000 h$^{-1}$ at 50 °C) was exhibited in the epoxidation of allylic alcohols with aqueous $H_2O_2$, which was attributed to the high degree of dispersion and good hydrothermal stability resulting from the confinement effect of the LDH layers. The catalyst could be readily recycled with no apparent loss of performance. Liu et al.[170] synthesized a novel PdMgAl-LDH catalyst intercalated by PWO for propene epoxidation by $O_2$ in methanol. High catalytic performance was observed because of not only the presence of highly active Pd particles in the brucite-like layers that generate $H_2O_2$ *in situ*, but also the strong epoxidation ability of the interlayer peroxo-POM in the presence of dilute $H_2O_2$, as well as the promotion effect of the basic layers on alkene epoxidation.

As well as intercalation in the interlayer galleries, anionic complexes can also be adsorbed on the external surfaces of LDH layers by taking advantage of their positive charge. For example Choudary and coworkers[171] immobilized a sulfonated chiral Mn(salen) complex onto MgAl-LDH and used the product as a catalyst for the asymmetric epoxidation of unfunctionalised olefins. Quantitative recovery was carried out by simple filtration and the catalyst was reused several times with negligible change in enantioselectivity and activity. The high stability was attributed to the spatial constraints imposed by the immobilization of the active phase on the LDH.

In summary, owing to their ability to impose a spatial confinement effect and their alkalinity, LDHs are gradually being employed in the design and synthesis of efficient and stable catalysts for epoxidation reactions. However, few studies have reported the application of LDHs as catalysts for gas-phase reactions, especially in the epoxidation of ethene which is the most significant example of industrial epoxidation. Therefore, we suggest that the application of LDH-based materials as catalysts for the epoxidation of ethene should become a focus of future research.

## 3.5 Elimination of NO$_x$ and SO$_x$ emissions

Sulfur and nitrogen oxides, two major pollutants emitted from diesel engines and fluid catalytic cracking (FCC) for power generation, have caused serious environmental problems, such as the formation of photochemical smog and acid rain, the depletion of the ozone layer and some human diseases.[172] As the legislation limits are becoming more and more stringent, developing practicable processes to control these contaminants is imperative.[173]

Recently developed technologies which have been successfully used to decrease NO$_x$ in the exhaust gases of thermal power stations include the continuously regenerating trap (CRT), selective catalytic reduction (SCR), as well as NO$_x$ storage and reduction (NSR).[174,175] Due to its high efficiency of NO$_x$ conversion, user-friendly control and low cost, NSR has become regarded as the most suitable technology for elimination of NO$_x$. The NSR method involves three processes: oxidization of NO to $NO_2$ by a reactive oxygen species, the storage of $NO_2$ and the reduction of adsorbed NO$_x$ by soot to $N_2$ and $CO_2$. Although numerous studies of NSR catalysts have been reported and theoretical models for NO$_x$ storage have been developed,[176] some problems still remain. Of these, the high temperatures required for NO$_x$ oxidation/reduction and the relatively low NO$_x$ storage capacity (NSC) are the most important. Thus, developing more active catalysts is clearly necessary. Cheng and coworkers[177] prepared a Pt doped MgAl-MMO catalyst for the removal of NO$_x$. Noble metal species were well dispersed on MgAl-MMO because of its large surface area and

the strong interaction between the Pt species and the support, which provided more active sites for converting NO to $NO_2$ and high NO$_x$ storage capability. The Mg/Al molar ratio in the Pt/MgAl-MMO catalyst was found to have a significant effect on the NO$_x$ storage capacity, with the catalyst having a Mg/Al molar ratio of 3 possessing the best performance for NO$_x$ storage. Similar Ru,[178] Ag,[179] and Pd[180] doped MgAl-MMO catalysts were also reported and the process of NO$_x$ removal over the RuMgAl-MMO catalyst is shown in Fig. 17.[178] In the RuMgAl-MMO catalytic system, the gaseous NO reacted with surface O to form $NO_2$, which then was stored at the basic sites nonadjacent to Ru species in the form of $NO_2^-/NO_3^-$. Li et al.[178] also investigated the influence of the treatment conditions on the $NO_2$ adsorption capacity and the stoichiometry of the adsorbed NO$_x$ species. The RuMgAl-MMO catalyst obtained after pretreatment at 350 °C exhibited the highest NO$_x$ storage capability of about 220 μmol g$^{-1}$ in a $N_2$ stream containing 790 ppm NO and 8% $O_2$.
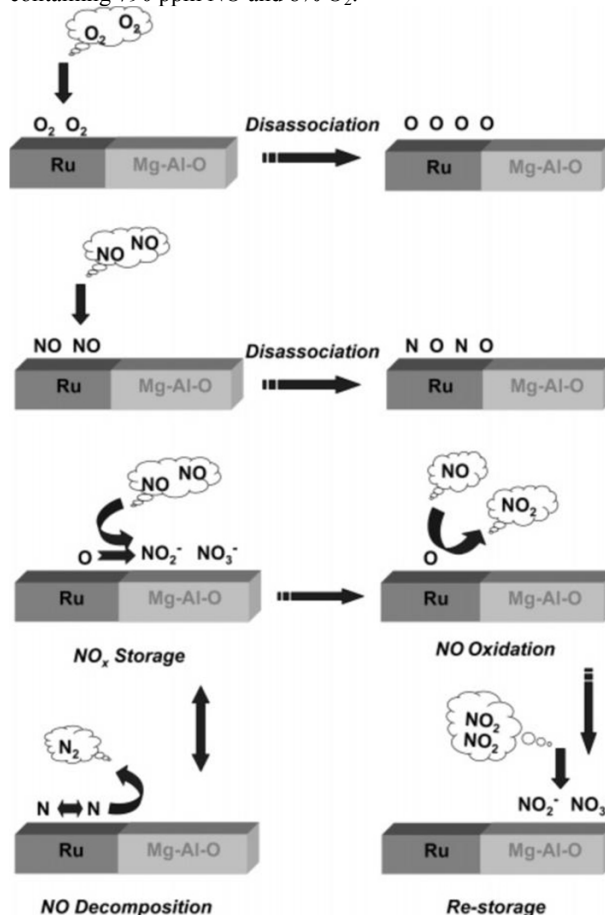


**Fig. 17** Proposed NO$_x$ storage/decomposition pathway on a Ru/MgAl-MMO catalyst. Reproduced with permission from ref. 178. Copyright 2007 American Chemical Society.

In addition to noble metal doped MgAl-MMO catalysts, non-noble catalysts have also attracted increasing attention and have been widely studied in De-NO$_x$ catalysis. In particular, catalysts containing different transition metals (e.g., Co, Cu, Ce) obtained from LDH precursors can either directly decompose NO$_x$ or effectively reduce NO$_x$ in the presence of excess $O_2$.[181] For example, Wang et al.[182] synthesized a CoAl-MMO catalyst derived from a binary CoAl-LDH precursor prepared by the co-precipitation method. The cobalt species proposed as the active sites were highly dispersed due to the inert $Al_2O_3$ effectively suppressed the migration and aggregation of Co oxides during the

calcination process. The calcination temperature of the LDH was found to have an effect on the catalytic properties, with both the activity and selectivity to $N_2$ of the catalyst calcined at 800 °C being higher than that calcined at 500 °C, mainly due to the enhanced redox properties of the cobalt species. The Co content was also found to have a significant influence on the catalytic performance. CoAl-MMO catalyst with a Co/Al ratio of 5 gave the highest selectivity to $N_2$ formation ($S[N_2]= 3.5\%$) at an ignition temperature ($T_i$) = 290 °C due to its intermediate basicity. The authors also studied[183-187] the catalytic removal of $NO_x$ over CuAl-MMO and CuMgAl-MMO catalysts derived from binary CuAl-LDH and ternary CuMgAl-LDH, respectively. CoMgAl-LDH derived catalysts have also been demonstrated to be very active for the catalytic removal of $NO_x$ but showed limited $NO_x$ storage ability.[188] Therefore, Ce was introduced into CoMgAl-LDH to afford CeCo oxide catalysts with both high oxidation ability and $NO_x$ storage ability.[189] In comparison with the Ce-free catalysts, a $Co_{2.5}Mg_{2.5}Al_{0.92}Ce_{0.08}$ catalyst exhibited higher performance, with temperature for maximal soot oxidation rate lowered significantly from 449 °C to 384 °C, increased $NO_x$ reduction (336 μmol g$^{-1}$ and 15.4%) as well as favorable $NO_x$ storage. This was interpreted in terms of the introduction of Ce increasing the dispersion of the main active phase $Co_3O_4$—which is regarded as the main active oxygen species for removal of $NO_x$.

It has been reported that an economical strategy for $SO_x$ elimination is the addition of $SO_x$ transfer additives to the FCC catalyst.[190] Compounds with intermediate basicity, such as MMOs derived from LDH precursors, are among the most promising transfer catalysts. For example, CoMgAl-MMO derived from LDHs with suitable basicity gave the optimal catalytic behavior required for the removal of $SO_2$.[191,192] In these catalysts, highly dispersed $Co_3O_4$ acted as active species for the removal of $SO_x$ since the redox properties of cobalt allow oxidation of $SO_2$ at high temperatures in the presence of oxygen. The removal of $SO_2$ over copper oxide catalysts derived from the corresponding LDH precursor was also investigated.[190-193] Compared with the catalyst obtained from the CoMgAl-LDH precursor, the Cu-containing sample exhibited higher catalytic behavior due to its stronger redox ability. In addition, the authors claimed that the regeneration of the Cu catalyst was also easier than that of the Co catalyst, due to the stronger interaction between Cu and support.

The above results indicate that the MMOs derived from LDH precursors could be used as both support and actual catalyst for the removal of $NO_x$ and $SO_x$. The MMO-based catalysts possess not only large surface area, a high dispersion of the active catalyst and appropriate redox properties to carry out the oxidation of $NO/SO_2$ to $NO_2/SO_3$, but also have intermediate basic properties which contribute to the effective $NO_x/SO_2$ storage ability. In addition, they also exhibit high stability and ease of regeneration due to the strong interactions between the different components and therefore have great potential for application as materials for the simultaneous removal of $SO_x$ and $NO_x$ in industrial emissions.

### 3.6 Selective oxidation of biomass

In the last decades, the price of fossil resource has risen dramatically due to the increased global demand and limited supply. Moreover, the extensive use of fossil resources also brings environmental problems. Therefore, the depletion of fossil feedstocks together with security of supply and environmental concerns have boosted the interest in the use of biomass as an alternative carbon source for heat and power, transportation fuels and chemicals.[194,195] However there are several issues that affect

the final replacement of fossil resource by biomass, such as the price of biomass products and efficient utilization.[196]

For example, biodiesel, which burns more cleaner, is expected to be a replacement for petroleum-based diesel.[197] However, glycerol is produced as a byproduct in the manufacture of biodiesel by transesterification of vegetable oils. The additional glycerol produced is currently almost double the present requirements.[198] If, as is likely, biodiesel production increases dramatically, there will be further overcapacity of crude glycerol. Therefore it is important to find ways of converting glycerol and homologous biomass products into value-added materials and thus enhance the economic benefits of biomass. As illustrated in Fig. 18, selective catalytic oxidation of glycerol gives six potential C3 oxygenated products together with C2 (oxalic acid) and C1 products.[199] These C3 products such as glyceric acid (GA) and tartronic acid, as well as oxalic acid, can be converted into various marketable products, e.g., polymers and biodegradable emulsifiers. In particular, GA can be used for the treatment of skin disorders, as an anionic monomer for the manufacture of packaging materials for volatile agents and biodegradable fabric softeners.[200-203] One of the key problems in glycerol oxidation is the potential complexity of the product mixture, therefore control of the reaction selectivity by careful design of the catalyst is required.
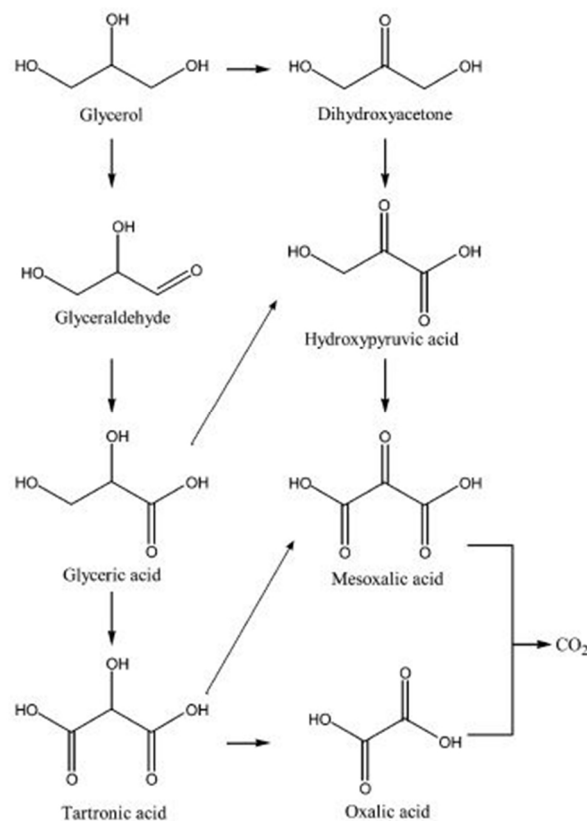


**Fig. 18** A possible reaction pathway for glycerol oxidation. Reproduced with permission from ref. 199. Copyright 2003 The Royal Society of Chemistry.

A great number of catalytic systems have been reported to be active in the oxidation of glycerol, but they are limited by the need to employ homogeneous bases. For example, Au-based catalysts are totally inactive in the oxidation of glycerol in the absence of the base NaOH.[204] Although GA in the form of its sodium salt can be obtained as the main product in the oxidation of glycerol under basic conditions, additional neutralization and acidification steps are required to obtain the free GA. From the viewpoint of

environmental and green chemistry, homogeneous bases should be avoided. By virtue of the basic character of LDH materials, LDH-supported metal catalysts have been widely studied in the selective oxidation of biomass and show the potential to replace homogeneous bases. For example, Ebitani and co-workers[205] prepared Au catalysts supported on commercial carbon and MgAl-LDH for the oxidation of glycerol. The results showed the Au/C catalyst possessed no activity in the absence of NaOH; the addition of base was essential due to the initial dehydrogenation involving proton abstraction from primary hydroxyl groups.[199] In contrast, Au/LDH could oxidize glycerol without NaOH and gave 100% glycerol conversion. This difference in catalytic performance over Au/C and Au/LDH catalysts clearly indicated that LDH, an efficient solid base support, had sufficient basicity for glycerol oxidation. They further investigated the effect of other active components supported on LDH: the catalytic activity for glycerol oxidation decreased in the order Pt/LDH > Au/LDH > Pd/LDH > Ru/LDH. The best catalyst, Pt NPs, was also immobilized on another basic support, $Mg(OH)_2$. Higher conversion (55%) with excellent selectivity to GA (75%) was achieved over Pt/LDH than that with $Pt/Mg(OH)_2$. In addition, the activity of the Pt/LDH was greatly influenced by the Mg/Al ratio of LDH; glycerol conversion increased (from traces to 56%) with increasing Mg/Al ratio (from 3 to 6). The selectivity to GA reached 70% when using the Pt/LDH with Mg/Al ratios of 5 and 6. Furthermore, the catalysts could be reused at least three times without loss of activity and selectivity. These results clearly indicated Pt/LDH affords excellent catalytic activity and yield of GA and is an effective catalyst for the selective oxidation of glycerol to GA in the absence of homogenous bases.

It is well-known that a synthesis method based on green chemistry principles not only involves careful design of the reaction pathway but also the use of environmentally friendly materials.[206-208] A green preparation of Pt NPs has been developed using soluble starch as a reducing and stabilizing agent and the Pt NPs were then immobilized on an MgAl-LDH surface.[209] The average particle size of Pt NPs and the loading of $Pt^0$ can be finely controlled by appropriate choice of reduction time (size: 0.9-2.1 nm; $Pt^0$ loading: 50-64%). These Pt/LDH catalysts were employed in the oxidation of glycerol in water using atmospheric molecular oxygen pressure. A Pt/LDH containing Pt NPs with a mean size of 1.9 nm and 61% $Pt^0$ loading was found to be the best catalyst, giving 41% yield and 75% selectivity for GA with a TON of 357. In addition, the Pt/LDH catalyst could be easily separated from the reaction mixture and was reusable three times. When the Pt/LDH was removed from the reaction mixture, no further oxidation took place, indicating the absence of metal leaching. Therefore, this Pt/LDH material is an environmentally friendly and highly efficient catalyst which suppresses the overoxidation of glycerol with molecular oxygen under atmospheric pressure and shows a great prospects for industrial application.

Because the synergistic effect between different metals in bimetallic NPs can give a superior catalytic performance, LDH-supported bimetallic catalysts were synthesized in attempt to enhance the efficiency of the oxidation of glycerol. Ebitani's group[210] prepared MgAl-LDH supported PtAu alloy nanoparticles with various Pt:Au molar ratios by a sol immobilization method, using soluble starch as a green reducing and stabilizing agent. All the catalysts, except for monometallic Au/LDH, promoted the selective oxidation of glycerol to GA with only minor amounts of tartronic acid, glycolic acid and oxalic acid being formed. The highest glycerol conversion (88%) was achieved using monometallic Pt/LDH, but this catalyst exhibited a low selectivity toward GA (48%). The positive synergistic effect of adding Au was

mainly reflected in the enhancement of selectivity. As the molar percentage of Au increased from 20 to 80, the activity gradually decreased, but overoxidation was suppressed and the selectivity for GA increased. Overall, the $Pt_{60}Au_{40}/LDH$ was the most effective catalyst with 57% yield of GA and a TOF of 84.7 $h^{-1}$ at room temperature. A possible mechanism for the oxidation of glycerol and other polyols by PtAu/LDH catalysts was proposed as shown in Fig. 19. Briefly, $O_2$ was activated by adsorption on a negatively charged Pt atom with electron transfer to the O-O $\pi^*$ antibonding orbital (step 1). Then the basic LDH support abstracted a proton from glycerol to form an alkoxide (step 2). Proton transfer from the alkoxide carbon atom to the adsorbed oxygen formed an aldehyde which is released (step 3) and the activated oxygen was regenerated (step 4). The aldehyde was then further oxidized to the carboxylic acid by an adsorbed activated oxygen species in a similar catalytic cycle (steps 5-8).
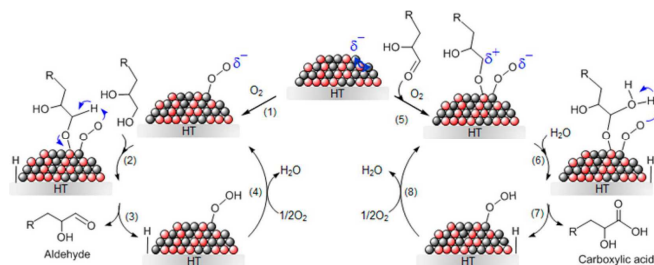


**Fig. 19** The proposed reaction mechanism for polyol oxidation catalyzed by PtAu/LDH (red spheres: Au, grey spheres: Pt.). Reproduced with permission from ref. 210. Copyright 2013 American Chemical Society.

5-Hydroxymethylfurfural (HMF) is also considered as a promising chemical for several industrial applications because it is available from biomass and can serve as the building block for many other molecules.[211,212] Similar to glycerol, selective oxidation is a key step in the conversion of HMF to added value products. One of the promising products obtained from HMF oxidation is 2,5-furandicarboxylic acid (FDCA), which is considered as one of the twelve most important biomass derived chemicals.[213] FDCA is regarded as a potential alternative for the terephtalic acid that is currently used for the preparation of polyethene terephthalate (PET).[191,214,215] Gupta et al.[216] reported an environmentally benign and safe process for FDCA synthesis using a Au/MgAl-LDH catalyst at 368 K under an ambient oxygen pressure without any addition of homogeneous base, whereas previous reports of the synthesis of FDCA or it dimethyl ester using gold catalysts on other supports required either addition of homogeneous base ($Au/CeO_2$) or a high-pressure reactor ($Au/TiO_2$). The Au/LDH catalyst afforded FDCA with >99% selectivity at total conversion of HMF when using ambient oxygen pressure. Even when using air instead of oxygen, high selectivity to FDCA (81%) was still achieved with total HMF conversion at 368 K. The activity of Au/LDH was much higher than those of $Au/Al_2O_3$, Au/C and $Au/SiO_2$, indicating that the basicity of the support plays an important role in the reaction. Furthermore, Au/LDH also exhibited higher activity than the more strongly basic Au/MgO catalyst, owing to the aggregation of Au NPs on the surface of MgO. The effect of varying the reaction temperature on the product distribution was also studied for Au/LDH. With increase of reaction temperature, the yield of FDCA increased, with a concomitant decrease in the yield of 5-hydroxymethyl-2-furancarboxylic acid (HMFCA). According to these results, a possible reaction mechanism was proposed. The oxidation of aldehyde groups of HMF to form corresponding monocarboxylic acid HMFCA occurred easily owing to the basicity of LDH. For

the synthesis of the FDCA, the rate-determining step was considered to be the oxidation of the hydroxyl group, which was also promoted by the basicity of the LDH. The basic sites of LDH contributed to the formation of intermediate hemiacetals from aldehydes (HMF and 5-formyl-2-furancarboxylic acid (FFCA)) and metal alcoholate species *via* a metal hydride shift from HMFCA. Takagaki and coworkers[217] demonstrated that Ru/MgAl-LDH afforded remarkable activity and selectivity for the conversion of HMF into 2,5-diformylfuran (DFF), which was used as a monomer for furan-based biopolymers and an intermediate in the manufacture of pharmaceuticals, antifungal agents and ligands.[218-220] Compared with Ru/Al$_2$O$_3$ and Ru/Mg(OH)$_2$, the Ru/LDH catalyst exhibited a higher yield of DFF (92%) with excellent selectivity (97%) when the reaction was carried out in oxygen. Even when using air, a 72% yield of DFF with 88% selectivity was achieved. However the direct synthesis of DFF from hexoses such as fructose and glucose was more desirable than synthesis from HMF because it avoided the need to separate and purify the intermediates and thus saved energy, time and solvents. Indeed, by using a combination of an MgAl-LDH as a solid base, Amberlyst-15 as a solid acid and Ru as the active metal. Takagaki and coworkers[217] showed it was possible to produce DFF effectively

from fructose and glucose via base-catalyzed isomerization, acid-catalyzed dehydration and successive selective oxidation in a one-pot reaction.

These studies highlight how selective oxidation is an effective method for utilization of biomass following the principles of green chemistry. Owing to the abundance of basic sites on the surface of LDH materials, it is can be used as a green replacement for the commonly used homogeneous bases. Careful design of the LDH-based catalysts can afford excellent catalytic performance under moderate conditions. Although further studies are needed, the LDH-supported catalysts have shown excellent potential for industrial application in the selective oxidation of biomass to obtain high-value organic compounds.

In conclusion, the supported catalysts based on LDHs materials have shown promising prospects in the field of petrochemical, fine chemicals, environmental protection and new energy. A summary of supported catalysts based on LDH/MMO materials used for the catalytic oxidation and hydrogenation reactions including the reaction type, conversion, target product and selectivity is presented in Table 1 to give a snapshot for the researchers in this field.

**Table 1** A summary of supported catalysts fabricated by using LDHs as supports/precursors for the catalytic oxidation and hydrogenation

| Reaction Type | Reaction | Catalyst | Temp. (K) | Conv. (%) | Target product | Sel. (%) | Ref. |
|---|---|---|---|---|---|---|---|
| Hydrogenation of C—C unsaturated bond | Acetylene hydrogenation | Tetrahedral Pd/MgAl-LDH | 353 | 90 | Ethene | 63 | 74 |
| | | Nanowire Pd/MgAl-LDH | 333 | 89 | | 62 | 75 |
| | | Pd-Ga(1:5)/MgO-Al$_2$O$_3$ | 318 | 85.9 | | 87.2 | 109 |
| | | PdAg/NiTi-LDH | 343 | 90 | | 82 | 144 |
| | | Nanoflower PdAu/MgAl-MMO | 393 | 91.2 | | 70 | 145 |
| | Dimethyl terephthalate hydrogenation | Pd/MgAl-MMO-Al$_2$O$_3$ | 453 | 96.0 | Dimethylcyclohexane-1,4-dicarboxylate (DMCD) | 98.5 | 148 |
| | | RuPd/MgAl-MMO-Al$_2$O$_3$ | 453 | 99.6 | | 96.1 | 149 |
| | DMCD hydrogenation | Cu/MgAl-MMO | 493 | 100 | 1,4-cyclohexanedimethanol | 99.8 | 150 |
| | 2-Butyne-1,4-diol hydrogenation | Pd/MgAl-MMO | 298-348 | 90 | 2-Butene-1,4-diol | 88 | 71 |
| | Phenylacetylene hydrogenation | Ni$_3$Ga/MgO | 313 | 95.1 | Styrene | 92.2 | 112 |
| | Styrene hydrogenation | NiCo (2:1)/Al$_2$O$_3$ | 333 | 99.0 | Ethylbenzene | >99.6 | 114 |
| | Citral hydrogenation | Pd/C$_{2.5}$-MgAl-LDH | 373 | 100 | Citronellal | 87.4 | 128 |
| Hydrogenation of C—O bond | CO$_2$ Methanation | Ni/Al$_2$O$_3$ | 573 | 99 | Methane | >99 | 152 |
| | | NiFe/Al$_2$O$_3$ | 493 | 58.5 | | 99.5 | 156 |
| | CO$_2$ hydrogenation | Cu/ZnAlZr-MMO | 523 | 23.9 | Methanol | 55.0 | 96 |
| | | PdGa/MgO | 523 | 1.0 | | 47 | 110 |
| | | PdZn/Al$_2$O$_3$ | 523 | 0.6 | | 60 | 110 |

| | | | | | | | |
|---|---|---|---|---|---|---|---|
| | Acetophenone hydrogenation | Arginine-mediated Pd/Mg$_3$Al-LDH | 358 | 97.0 | 1-Phenyl ethanol | 100 | 73 |
| | Glucose hydrogenation | Pt/MgAl-MMO | 363 | 80 | Sorbitol and Mannitol | (Yield) 39 | 58 |
| | Xylose hydrogenation | Pt/MgAl-MMO | 333 | 59 | Xylitol | (Yield) 50 | 58 |
| | Phenylethanal hydrogenation | Ni$_3$In/Al$_2$O$_3$ | 393 | 81 | 1-phenylethanol | 99 | 111 |
| | Cinnamaldehyde hydrogenation | Pt/MgAl-LDH | 333 | 79.7 | Cinnamyl alcohol | 85.4 | 82 |
| | | CuMgAl-MMO | 433 | 51.0 | | 20.8 | 120 |
| | Citral hydrogenation | Ni-ZnO/C | 413 | 100 | Citronellol | 92.3 | 103 |
| Alcohol oxidation | Benzyl alcohol oxidation | Au/MgAl-LDH | 353 | 89 | Benzaldehyde | 93 | 37 |
| | | Flower-like Au/NiAl-LDH | 373 | 53 | | 99 | 41 |
| | | Pd/Mg$_3$Al-LDH | 338 | 98 | | (Yield) 98 | 50 |
| | | Diamine functionalized Pd/Zn$_3$Al-LDH | 338 | 94 | | 100 | 53 |
| | | PdAu/Mg$_2$Al-LDH | 413 | 93 | | 93 | 59 |
| | | Mn/MgAl-LDH | 373 | 99 | | (Yield) 99 | 60 |
| | 1-Phenylethanol oxidation | Au/MgAl-LDH | 313 | 99 | Phenylethanal | (Yield) 99 | 36 |
| | | Au/Ni$_3$Al-LDH | 353 | 85.3 | | 99 | 40 |
| | | Pd/Mg$_3$Al-LDH | 338 | 80 | | (Yield) 75 | 50 |
| | | Fe$_3$O$_4$@MgAl-LDH@Au | 353 | - | | (Yield) 99 | 48 |
| | Glycerol oxidation | Au/Mg$_5$Al-LDH | 293 | 78 | Glycolic acid | 53 | 39 |
| | | Pt/Mg$_5$Al-LDH | 333 | 55 | Glyceric acid | 75 | 209 |
| | | Pt$_{60}$Au$_{40}$/Mg$_5$Al-LDH | 298 | 73 | | 78 | 210 |
| | 5-Hydroxymethylfurfural oxidation | Au/Mg$_5$Al-LDH | 368 | >99 | 2,5-Furandicarboxylic acid | >99 | 216 |
| | | Ru/Mg$_3$Al-LDH | 393 | - | 2,5-Diformylfuran | (Yield) 92 | 217 |
| Methane oxidation | | Ni/CaAl-MMO | 1073 | 95.3 | CO | 97.5 | 90 |
| | | Ru/MgAl-MMO | 1023 | 96 | | 95 | 97 |
| Epoxidation of olefins | Epoxidation of phenol red | NiAl-WO$_4^{2-}$-LDH | 298 | 100 | Bromophenol blue | 100 | 159 |
| | Epoxidation of Propene | PdMgAl-[PW$_{11}$O$_{39}$]-LDH | 353 | 47.5 | Propene oxide | 91.5 | 170 |

| | | | | | | | |
|---|---|---|---|---|---|---|---|
| Elimination of $NO_x$ and $SO_x$ emissions | | Pt/MgAl-MMO | 573 | 60 | $NO_2$ | - | 177 |
| | | Pd/MgAl-MMO | 573 | 90 | | - | 180 |
| | | CoMgAl-MMO | 1023 | 92 | $SO_3$ | - | 188 |
| Tandem reaction | Oxidative lactonization of 1,4-butanediol | Au/MgAl-LDH | 353 | 99 | γ-Butyrolactone | (Yield) 99 | 35 |
| | Oxidative esterification of benzyl alcohol | Au/Mg$_5$Al-LDH | 333 | 98 | Methyl benzoate | >99 | 38 |
| | Oxidative coupling of 1-hexylamine and benzyl alcohol | Au/Mg$_2$Al-LDH | 333 | 95 | Imine | 97 | 38 |
| | Condensation and selective hydrogenation of acetone | Pd/MgAl-MMO | 391 | 38.0 | Methyl isobutyl ketone | 82.2 | 78 |
| | Condensation and selective hydrogenation of acetone | Pt/MgAl-MMO | 391 | 34.0 | Methyl isobutyl ketone | 52.4 | 78 |

## 4. Conclusions and perspectives

Catalysis plays a prominent role in science and the chemical industry as it enables the preparation of chemicals and materials in an atom economical and efficient manner. Catalytic oxidation and hydrogenation, as fundamental reactions in the manufacture of a wide range of chemicals has attracted considerable interest in terms of both fundamental research and industrial applications. Because of their easy separation and recyclability, supported catalysts are widely used in these two processes. LDHs offer the advantages of the layered structure, compositional diversity, high stability, ease of preparation and low cost and have promising prospects for the design and synthesis of novel supported catalysts. This review has provided an overview of the recent progress in studies of supported catalysts based on LDH materials for use in catalytic hydrogenation and oxidation. The high adsorption capacity and cation-tunability of the brucite-like layers allows a wide range of supported catalysts to be fabricated by immobilizing the desired catalytically active species onto the surface of various LDHs and their calcined products (MMOs). Tunable surface basicity and acidity provides many opportunities for the synthesis of metal-alkali/acid multifunctional catalysts. The uniform dispersion of metallic cations in the layers and the oriented arrangement of anions in the interlayer galleries make LDHs a promising catalyst precursor for the formation of supported catalysts with a high degree of dispersion of the active material. Meanwhile, the topological transformation of the LDH precursor by calcination/reduction results in the formation of many defect sites and strong interactions between the active components and the concomitantly formed substrate, which prevents the aggregation/sintering of the active species and thus improves the stability. Furthermore, the assembly or hybridization of LDHs with different materials to form composites with hierarchical structures improves the functionality of the catalysts and therefore further enhances the catalytic performance due to the synergistic effects.

Partial hydrogenation of acetylene, hydrogenation of DMT, methanation, epoxidation of olefins, elimination of $NO_x$ and $SO_x$ emissions and selective oxidation of biomass have been chosen as representative reactions in the petrochemical, fine chemicals, environmental protection and clean energy fields to highlight the potential applications of LDH-based catalysts in catalytic oxidation and hydrogenation. The most important advantages of LDHs as precursors to supported catalysts for selective hydrogenation of acetylene and DMT, as well as methanation, are the ability to introduce the active cations into the layers of LDHs to achieve a uniform dispersion isolated by other inert cations and the strong interaction between the active component and the support after calcination and reduction, which enhances both catalytic activity and stability. Due to the abundance of basic sites on the surface of LDHs and their synergistic interaction with the metallic sites, it is possible to replace the commonly used homogeneous base in the oxidation of biomass to form high-value organic compounds following the principles of green chemistry. In addition to their alkalinity, another key advantage of LDHs in epoxidation reactions using POM catalysts is the anchoring effect of the interlayer gallery on the active POM component, which inhibits deactivating dimerization or self-oxidation reactions of the active species. MMO materials formed by the topotactic transformation of LDHs are promising bifunctional catalysts for the elimination of $NO_x$ and $SO_x$ by virtue of the high dispersion of surface redox species affording high activity for the conversion of $NO_x$ and $SO_x$ as well as the abundance of basic sites leading to an increase in storage capability.

Although considerable progress in the design and synthesis of supported catalysts derived from LDH materials with the functionality required to meet the different requirements of oxidation and hydrogenation has been obtained, there are still some issues that need to be addressed: (i) In terms of the use of LDHs as a support, although the formation of smaller particles of the active phases can be achieved on the surface of LDHs compared to other supports, the reasons for this need to be further investigated. Additionally, the effect of the nature of the LDH on the shape, exposed facets and the contact angle of active phase needs to be further explored, since this is also important for the design and synthesis of high performance LDH-supported catalysts. (ii) As for the utilization of LDHs as a catalyst precursor, the confinement effect of the LDHs on the catalytically active species deserves deeper study by in-situ monitoring of the topotactic transformation of LDH precursors into supported catalysts. (iii) Despite the numerous publications reporting the preparation of supported multimetallic catalysts using the LDH precursor method, a systematic study of the effect of the LDH properties on the structure of the active components—especially the extent of alloying—is lacking. (iv) The fabrication of hierarchical LDH-based composites, especially hybrids involving supports widely used in the chemical industry—such as molecular sieves and

SiO$_2$—is worthy of further study, since this offers a way to obtain a wide variety of multifunctional catalysts with enhanced catalytic performance and ease of recyclability by virtue of the synergy between the LDH and the other material. (v) On the basis of the excellent performance of LDH-based supported catalysts in both oxidation and hydrogenation processes, future studies should focus on the design and synthesis of LDH-based catalysts for the coupling reactions involved with these two kinds of processes. We believe overcoming the above challenges will make great contributions to the development of new practical supported catalysts based on LDH materials for both oxidation and hydrogenation reactions.

## Acknowledgements

## Notes and references

1 F. Zaera, *Chem. Soc. Rev.,* 2013, **42**, 2746.

2 Y. Sun, S. Gao, F. Lei and Y. Xie, *Chem. Soc. Rev.*, 2015, **44**, 623.

3 Z. Guo, B. Liu, Q. Zhang, W. Deng, Y. Wang and Y. Yang, *Chem. Soc. Rev.,* 2014, **43**, 3480.

4 N. López and C. Vargas-Fuentes, *Chem. Commun.*, 2012, **48**, 1379.

5 T. Mitsudome and K. Kaneda, *Green Chem.*, 2013, **15**, 2636.

6 F. Wang, C. Li, L. D. Sun, C. H. Xu, J. Wang, J. C. Yu and C. H. Yan, *Angew. Chem.*, 2012, **124**, 4956.

7 R. J. White, R. Luque, V. L. Budarin, J. H. Clark and D. J. Macquarrie, *Chem. Soc. Rev.,* 2009, **38**, 481.

8 L. Kesavan, R. Tiruvalam, M. H. Ab Rahim, M. I. bin Saiman, D. I. Enache, R. L. Jenkins, N. Dimitratos, J. A. Lopez-Sanchez, S. H. Taylor, D. W. Knight, C. J. Kiely and G. J. Hutchings, *Science*, 2011, **331**, 195.

9 Y. Li and W. J. Shen, *Chem. Soc. Rev.*, 2014, **43**, 1543.

10 J. P. Wilcoxon and B. L. Abrams. *Chem. Soc. Rev.*, 2006, **35**, 1162.

11 M. Sankar, N. Dimitratos, P. J. Miedziak, P. P. Wells, C. J. Kiely and G. J. Hutchings, *Chem. Soc. Rev.*, 2012, **41**, 8099.

12 F. Cavani, F. Trifirü and A. Vaccari, *Catal. Today*, 1991, **11**, 173.

13 P. J. Sideris, U. G. Nielsen, Z. Gan and C. P. Grey, *Science*, 2008, **321**, 113.

14 D. G. Evans and R. C. T. Slade, *Struct. Bond.*, 2006, **119**, 1.

15 L. Desigaux, M. B. Belkacem, P. Richard, J. Cellier, P. Leone, L. Cario, F. Leroux, C. T. Gueho and B. Pitard, *Nano Lett.*, 2006, **6**, 199.

16 M. Fogg, A. L. Rohl, G. M. Parkinson and D. Oʹ Hare, *Chem. Mater.*, 1999, **11**, 1194.

17 S. Nishimura, A. Takagaki and K. Ebitani, *Green Chem.*, 2013, **15**, 2026.

18 J. C. A. A. Roelofs, D. J. Lensveld, A. J. van Dillen and K. P. de Jong, *J. Catal.*, 2001, **203**, 184.

19 J. T. Feng, Y. J. Lin, D. G. Evans, X. Duan and D. Q. Li, *J. Catal.*, 2009, **266**, 351.

20 X. X. Guo, F. Z. Zhang, D. G. Evans and X. Duan, *Chem. Commun.,* 2010, **46**, 5197.

21 S. He, Z. An, M. Wei, D. G. Evans and X. Duan, *Chem. Commun.*, 2013, **49**, 5912.

22 Z. P. Xu, J. Zhang, M. O. Adebajo, H. Zhang and C. H. Zhou, *Appl. Clay Sci.* 2011, **53**, 139.

23 G. L. Fan, F. Li, D. G. Evans and X. Duan, *Chem. Soc. Rev.*, 2014, **43**, 7040.

24 X. Xiang, H. I. Hima, H. Wang, and F. Li, *Chem. Mater.* 2008**, 20**, 1173.

25 R. Dinka, K. Prandová and M. Hronec, *Appl. Clay Sci.*, 1998, **13**, 467.

26 A. Noujima, T. Mitsudome, T. Mizugaki, K. Jitsukawa and K. Kaneda, *Angew. Chem., Int. Ed.***,** 2011, **50**, 2986.

27 T. Chen, F. Zhang and Y. Zhu. *Catal. Lett.*, 2013, **143**, 206.

28 L. Li, L. Dou and H. Zhang, *Nanoscale*, 2014, **6**, 3753.

29 F. Prinetto, D. Tichit, R. Teissier and B. Coq, *Catal. Today,* 2000, **55**, 103.

30 B. M. Choudary, M. L. Kantam, V. Neeraja, K. K. Rao, F. Figueras and L. Delmotte, *Green Chem.,* 2001, **3**, 257.

31 Y. Xi and R. J. Davis, *J. Catal.,* 2008, **254**, 190.

32 W. Fang, J. Chen, Q. Zhang, W. Deng and Y. Wang, *Chem.Eur. J.*, 2011, **17**, 1247..

33 G. J. Hutchings, *J. Catal.,* 1985, **96**, 292.

34 S. E. Davis, M. S. Ide and R. J. Davis, *Green Chem.*, 2013, **15**, 17.

35 T. Mitsudome, A. Noujima, T. Mizugaki, K. Jitsukawa, K. Kaneda, *Green Chem.*, 2009, **11**, 793

36 T. Mitsudome, A. Noujima, T. Mizugaki, K. Jitsukawa and K. Kaneda, *Adv. Synth. Catal.*, 2009, **351**, 1890.

37 L. Wang, J. Zhang, X. J. Meng, D. F. Zheng, F. S. Xiao, *Catal. Today*, 2011, **175**, 404.

38 P. Liu, C. Li and E. J. M. Hensen, *Chem. Eur. J.*, 2012, **18**, 12122.

39 A. Takagaki, A. Tsuji, S. Nishimura and K. Ebitani, *Chem. Lett.*, 2011, **40**, 150.

40 L. Li, L. G. Dou and H. Zhang, *Nanoscale*, 2014, **6**, 3753.

41 Y. Y. Du, Q. Jin, J. T. Feng, N. Zhang, Y. F. He and D. Q. Li, *Catal. Sci. Technol.*, DOI:10.1039/c5cy00160a.

42 P. Liu, V. Degirmenci and E. J. M. Hensen, *J. Catal.*, 2014, **313**, 80.

43 L. Li, Q. Chen, Q. Zhang, J. J. Shi, Y. S. Li, W. R. Zhao and J. L. Shi, *Catal. Commun.*, 2012, **26**, 15.

44 S. X. Xia, L. P. Zheng, W. S. Ning, L. N. Wang, P. Chen and Z. Y. Hou, *J. Mater. Chem. A*, 2013, **1**, 11548.

45 H. Zhang, G. Y. Zhang, X. Bi and X. T. Chen, *J. Mater. Chem. A*, 2013, **1**, 5934.

46 L. Zhou, C. Gao and W. Xu, *Langmuir*, 2010, **26**, 11217.

47 S. W. Lee, J. Drwiega, C. Y. Wu, D. Mazyck and W. M. Sigmund, *Chem. Mater.*, 2004, **16**, 1160.

48 F. Mi, X. T. Chen, Y. W. Ma, S. T. Yin, F. L. Yuan and H. Zhang, *Chem. Commun.*, 2011, **47**, 12804.

49 T. Nishimura, N. Kakiuchi, M. Inoue and S. Uemura, *Chem. Commun.*, **2000**, 1245.

50 N. Kakiuchi, Y. Maeda, T. Nishimura and S. Uemura, *J. Org. Chem.*, 2001, **66**, 6620.

51 T. Chen, F. Z. Zhang and Y. Zhu, *Catal. Lett.*, 2013, **143**, 206.

52 P. Li, C. He, J. Cheng, C. Y. Ma, B. J. Dou and Z. P. Hao, *Appl. Catal., B*, 2011, **101**, 570.

53 M. Sahoo and K. M. Parida, *Appl. Catal., A*, 2013, **460-461**, 36.

54 K. Motokura, D. Nishimura, K. Mori, T. Mizugaki, K. Ebitani, and K. Kaneda, *J. Am. Chem. Soc.* 2004, **126**, 5662

55  C. S. Cho, B. T. Kim, T. J. Kim and S. C. Shim, *Chem. Commun.,* 2001, 2576.55

56 C. S. Cho, B. T. Kim, H. J. Choi and T. J. Kim, S. C. Shim, *Tetrahedron,* 2003, **59**, 7997.

57 K. Motokura, T. Mizugaki, K. Ebitani and K. Kaneda, *Tetrahedron Lett.*, 2004, **45**, 6029.

58  A. Tathod, T. Kane, E. S. Sanil and P. L. Dhepe, *J. Mol. Catal. A: Chem.*, 2014, **388-389**, 90.

59  J. T. Feng, C. Ma, P. J. Miedziak, J. K. Edwards, G. L. Brett, D. Q. Li, Y. Y. Du, D. J. Morgan and G. J. Hutchings, *Dalton Trans.*, 2013, **42**, 14498

60  K. Nagashima, T. Mitsudome, T. Mizugaki, K. Jitsukawa and K. Kaneda, *Green Chem.*, 2010, **12**, 2142.

61  M. L. Kantam, B. V. Prakash, B. Bharathi and C. V. Reddy, *J. Mol. Catal. A: Chem.*, 2005, **226**, 119.

62  Z. Y. Sun, L. Jin, Y. F. Zhao, S. He, S. D. Li, M. Wei and L. R. Wang, *Ind. Eng. Chem. Res.*, 2014, **53**, 4595.

63  Z. Y. Sun, L. Jin, S. He, Y. F. Zhao, M. Wei, D. G. Evans and X. Duan, *Green Chem.*, 2012, **14**, 1909.

64  F. Kovanda and K. Jirátová, *Catal. Today*, 2011, **176**, 110.

65  J. T. Feng, X. Y. Ma, Y. F. He, D. G. Evans and D. Q. Li, *Appl. Catal., A,* 2012, **413**, 10.

66  M. L. Kantam, T. Parsharamulu, S.V. Manorama, *J. Mol. Catal. A: Chem.*, 2012, **36**, 115.

67  J. C. A. A. Roelofs and P. H. Berben, *Chem. Commun.,* 2004, 970.

68  F. Iosif,  V. I. Parvulescu, M. E. P. Bernalb, R. J. R. Casero, V. Rives, K. Kranjc, S. Polanc, M. Kočevarc, E. Genind, J. P. Genêt, V. Michelet, *J. Mol. Catal. A: Chem.*, 2007, **276**, 34.

69  P. Sangeetha, K. Shanthi, K. S. R. Rao, B. Viswanathanc and P. Selvam, *Appl. Catal., A*, 2009, **353**,160.

70  A. H. Padmasri, A. Venugopal, V. Siva Kumar, V. Shashikala, B. M. Nagaraja, P. Seetharamulu, B. Sreedhar, B. D. Raju, P. K. Rao and K. S. R. Rao, *J. Mol. Catal. A: Chem.*, 2004, **223**, 329.

71  D. Francová, N. Tanchoux, D. Tichit, B. Coq, P. Trens, F. Prinetto and G. Ghiotti, *Micropor. Mesopor. Mat.*, 2007, **99**, 118.

72  P. Sangeetha, P. Seetharamulu, K. Shanthi, S. Narayanan and K. S. R. Rao, *J. Mol. Catal. A: Chem.*, 2007, **273**, 244.

73  R. T. Tao, Y. Xie, G. M. An, K. L. Ding, H. Y. Zhang, Z. Y. Sun and Z. M. Liu, *J. Colloid Interf. Sci.*, 2010, **351**, 501.

74  J. T. Feng, X. Y. Ma, Y. F. He, D. G. Evans and D. Q. Li, *Appl. Catal. A: Gen.*, 2012, **413-414**, 10.

75  Y. F. He, J. T. Feng, Y. Y. Du and D. Q. Li, *ACS Catal.*, 2012, **2**, 1703.

76  X. Y. Ma, Y. Y. Chai, D. G. Evans, D. Q. Li and J. T. Feng, *J. Phys. Chem. C*, 2011, **115**, 8693.

77  J. T. Feng, X. Y. Ma, D. G. Evans and D. Q. Li, *Ind. Eng. Chem. Res.,* 2011, **50**, 1947.

78  A. A. Nikolopoulos, B. W. L. Jang and J. J. Spivey, *Appl. Catal., A*, 2005, **296**, 128.

79  F. Winter, M. Wolters, A. J. van Dillen and K. P. de Jong, *Appl. Catal., A*, 2006, **307**, 231.

80  K. Motokura, N. Fujita, K. Mori, T. Mizugaki, K. Ebitani and K. Kaneda, *Tetrahedron Lett.*, 2005, **46**, 5507.

81  D. Tichit, M. de J. M. Ortiz, D. Francová, C. Gérardin, B. Coq, R. Durand, F. Prinetto and G. Ghiotti, *Appl. Catal., A*, 2007, **318**, 170.

82  X. Xiang, W. H. He, L. S. Xie and F. Li, *Catal. Sci. Technol.*, 2013, **3**, 2819

83  Y. T. Tsai, X. H. Mo, A. Campos, J. G. Goodwin Jr. and J. J. Spivey, *Appl. Catal., A*, 2011, **396** 91.

84  A. Kogelbauer, J. G. Goodwin Jr. and R. Oukaci, *J. Catal.*, 1996, **160**, 125.

85 A. R. Belambe, R. Oukaci and J. G. Goodwin Jr., *J. Catal.*, 1997, **166**, 8.

86  S. Albertazzi, G. Busca, E. Finocchio, R. Glöckler and A. Vaccari, *J. Catal.*, 2004, **223**, 372.

87  W. Huang, J. R. McCormick, R. F. Lobo and J. G. Chen, *J. Catal.,* 2007, **246**, 40.

88  J. A. Lopez-Sanchez, N. Dimitratos, C. Hammond, G. L. Brett, L. Kesavan, S. White, P. Miedziak, R. Tiruvalam, R. L. Jenkins, A. F. Carley, D. Knight, C. J. Kiely and G. J. Hutchings, *Nature Chem.*, 2011, **3**, 551.

89 Z. Jiang, J. Yu, J. Cheng, T. Xiao, M. O. Jones, Z. Hao and P. P. Edwards, *Fuel Proc.Technol.*, 2010, **91**, 97.

90 H. Morioka, Y. Shimizu, M. Sukenobu, K. Ito, E. Tanabe, T. Shishido and K. Takehira, *Appl. Catal., A*, 2001, **215**, 11.

91  D. Tichit, R. Durand, A. Rolland, B. Coq, J. Lopez and P. Marion, *J. Catal.*, 2002, **211**, 511.

92  N. T. Dung, D. Tichit, B. H. Chiche and B. Coq, *Appl. Catal., A*, 1998, **169**, 179.

93  F. M. Cabello, D. Tichit, B. Coq, A. Vaccari and N. T. Dung, *J. Catal.*, 1997, **167**, 142.

94  D. Tichit, F. Medina, R. Durand, C. Mateo, B. Coq, J. E. Suerias and P. Salagre, in "Heterogeneous Catalysis and Fine Chemicals IV" (H.U. Blaser, A. Baiker and R. Prins, Eds.), p. 297. Elsevier, Amsterdam, 1997.

95  L. H. Huang, J. Zhou, A. T. Hsu and R. R. Chen, *Int. J. Hydrogen Energ.*, 2013, **38**, 14550.

96  P. Gao, F. Li, F. Xiao, N. Zhao, N. Sun, W. Wei, L. Zhong and Y. Sun, *Catal. Sci. Technol.*, 2012, **2**, 1447.

97  A. Ballarini, P. Benito, G. Fornasari, O. Scelza and A. Vaccari, *Int. J. Hydrogen Energ.*, 2013, **38**, 15128.

98  X. Wen, R. S. Li, Y. X. Yang, J. L. Chen and F. Z. Zhang, *Appl. Catal., A*, 2013, **468**, 204.

99  S. X. Xia, W. C. Du, L. P. Zheng, P. Chen and Z. Y. Hou, *Catal. Sci. Technol.*, 2014, **4**, 912.

100  R. F. Xie, G. L. Fan, Q. Ma, L. Yang and F. Li, *J. Mater. Chem. A*, 2014, **2**, 7880.

101  J. Wang, G. L. Fan and F. Li, *RSC Adv.*, 2012, **2**, 9976.

102  J. Wang, G. L. Fan and F. Li, *Catal. Sci. Technol.*, 2013, **3**, 982.

103  L. Yang, Z. S. Jiang, G. L. Fan and F. Li,*Catal. Sci. Technol.*, 2014, **4**, 1123

104  M. Y. Miao, J. T. Feng, Q. Jin, Y. F. He, Y. N. Liu, Y. Y. Du, N. Zhang and D. Q. Li, *RSC Adv.*, 2015, **5**, 36066

105  D. S. Wang and Y. D. Li, *Adv. Mater.*, 2011, **23**, 1044.

106  M. Jaime, R. Movshovich, G. R. Stewart, W. P. Beyermann, M. G. Berisso, M. F. Hundley, P. C. Canfield and J. L. Sarrao, *Nature*, 2000, **405**, 160.

107   B. D. Adams, G. Wu, S. Nigro and A. Chen, *J. Am. Chem. Soc.*, 2009, **131**, 6930.

108   R. Ferrando, J. Jellinek and R. L. Johnston, *Chem. Rev.*, 2008, **108**, 845.

109   Y. F. He, L. L. Liang, Y. N. Liu, J. T. Feng, C. Ma and D. Q. Li, *J. Catal.,* 2014, **309**, 166.

110   A. Ota, E. L. Kunkes, I. Kasatkin, E. Groppo, D. Ferri, B. Poceiro, R. M. N. Yerga and M. Behrens, *J. Catal.*, 2012, **293**, 27.

111   C. M. Li, Y. D. Chen, S. T. Zhang, S. M. Xu, J. Y. Zhou, F. Wang, M. Wei, D. G. Evans and X. Duan, *Chem. Mater.*, 2013, **25**, 3888.

112   C. Li, Y. Chen, S. Zhang, J. Zhou, F. Wang, S. He, M. Wei, D. G. Evans and X. Duan, *ChemCatchem*, 2014, **6**, 824.

113   B. Coq, D. Tichit and S. Ribet, *J. Catal.*, 2000, **189**, 117.

114   J. F. Xiang, X. Wen and F. Z. Zhang, *Ind. Eng. Chem. Res.*, 2014, **53**, 15600.

115   B. Dragoi, A. Ungureanu, A. Chirieac, C. Ciotonea, C. Rudolf, S. Royer and E. Dumitriu, *Appl. Catal., A,* 2014, http://dx.doi.org/10.1016/ 2014.11.016.

116   A. Urdă, I.Popescu, T. Cacciaguerra, N. Tanchoux, D. Tichit and I. C. Marcu, *Appl. Catal., A*, 2013, **464-46**5, 20.

117   S. Tanasoi, G. Mitran, N. Tanchoux, T. Cacciaguerra, F. Fajula, I. Šandulescu, D. Tichit and I. C. Marcu, *Appl. Catal., A*, 2011, **395**, 78.

118   S. D. Li, H. S. Wang, W. M. Li, X. F. Wu, W. X. Tang,Y. F. Chen, *Appl. Catal., B*, 2015, **166-167**, 260.

119   R. F. Xie, G. L. Fan, L. Yang and F. Li, ,*Catal. Sci. Technol.*, 2015, **5**, 540

120   J. Barrault, A. Derouault, G. Courtois, J. M. Maissant, J. C. Dupin, C. Guimonb, H. Martinez and E. Dumitriu, *Appl. Catal., A*, 2004, **262**, 43.

121   L. C. Meher, R. Gopinath, S. N. Naik and A. K. Dalai, *Ind. Eng. Chem. Res.*, 2009, **48**, 1840.

122   Mori, H. Abet and S. Inoue, *Appl. Organomet. Chem.*, 1995, **9**, 189.

123   C. Gérardin, D. Kostadinova, N. Sanson, B. Coq and D. Tichit, *Chem. Mater.,* 2005, **17**, 6473.

124   M. Q. Zhao, Q. Zhang, W. Zhang, J. Q. Huang, Y. H. Zhang, D. S. Su and F. Wei, *J. Am. Chem. Soc.*, 2010, **132**, 14739.

125   W. M. Lv, L. Yang, B. B. Fan, Y. Zhao, Y. F. Chen, N. Y. Lu and R. F. Li, *Chem. Eng. J.*, 2015, **263**, 309.

126   Z. Chang, N. Zhao, J. F. Liu, F. Li, D. G. Evans, X. Duan, C. Forano and M. De Roy, *J. Solid State Chem.*, 2011, **184**, 3232.

127   M. Raciulete, G. Layrac, D. Tichit and I. C. Marcu, *Appl. Catal., A*, 2014, **477**, 195.

128   R. R. Han, C. S. Nan, L. Yang, G. L. Fan and F. Li, *RSC Adv.*, 2015, **5**, 33199

129   M. Lan, G. L. Fan, Y. H. Wang, L. Yang and F. Li,, *J. Mater. Chem. A*, 2014, **2**, 14682.

130   N. Barrabés, A. Frare, K. Föttinger, A. Urakawa, J. Llorca, G. Rupprechter and D. Tichit, *Appl. Clay Sci.*, 2012, **69**, 1.

131   D. H. Mei, M. Neurock and C. M. Smith, *J. Catal.*, 2009, **268**, 181.

132   Y. P. G. Chua, G. T. K. K. Gunasooriya, M. Saeys and E. G. Seebauer, *J. Catal.*, 2014, **311**, 306.

133   S. Komhoma, O. Mekasuwandumrong, P. Praserthdam and J. Panpranot, *Catal. Commun.*, 2008, **10**, 86.

134   A. Borodzinski and G. C. Bond, *Catal. Rev. Sci. Eng.*, 2008, **50**, 379.

135   D. P. Mei, A. Sheth, M. Neurock and C. M. Smith, *J. Catal.*, 2006, **242**, 1.

136  .N. Ló pez and C. V. Fuentes, *Chem. Commun.*, 2012, **48**, 1379.

137   W. Huang, W. Pyrz, R. F. Lobo and J. G. Chen, *Appl. Catal.* A: Gen.*,* 2007, **333**, 254.

138   M. J. Vincent and R. D. Gonzalez, *Appl. Catal.,* A, 2001, **217**, 143.

139   S. Asplund, *J. Catal.,* 1996, **158**, 267.

140   I. Y. Ahn, J. H. Lee, S. S. Kum and S. H. Moon, *Catal. Today,* 2007, **123**, 151.

141   I. Y. Ahn, J. H. Lee, S. K. Kim and S. H. Moon, *Appl. Catal., A*, 2009, **360**, 38.

142   L. D. Meng and G. C. Wang, *Phys. Chem. Chem. Phys.*, 2014, **16**, 17541.

143   A. Borodzinski and G. C. Bond, *Catal. Rev.,* 2008, **50**, 379.

144   Y. Liu, J. Feng, Y. He, J. Sun and D. Li, *Catal. Sci. Technol.*, 2015, **5**, 1231.

145   C. Ma, Y. Y. Du, J. T. Feng, X. Z. Cao, J. Yang and D. Q. Li, *J. Catal.*, 2014, **317**, 263.

146   A. Ota, J. Kröhnert, G. Weinberg, I. Kasatkin, E. L. Kunkes, D. Ferri, F. Girgsdies, N. Hamilton, M. Armbrüster, R. Schlögl and M. Behrens, *ACS Catal.*, 2014, **4**, 2048.

147   A. B. Hungria, R. Raja, R. D. Adams, B. Captain, J. M. Thomas, P. A. Midgley, V. Golovko and B. F. G. Johnson, *Angew. Chem. Int. Edit.*, 2006, **45**, 4782.

148   F. Z. Zhang, J. L. Chen, P. Chen, Z. Y. Sun and S. L. Xu, *AIChE J.*, 2012, **58**, 1853.

149   J. L. Chen, L. Guo and F. Z. Zhang, *Catal. Commun.*, 2014, **55**, 19.

150   S. Y. Zhang, G. L. Fan and F. Li, *Green Chem.,* 2013, **15**, 2389.

151   Q. Hu, G. L. Fan, S. Y. Zhang, L.Yang, F. Li, *J. Mol. Catal. A: Chem.*, 2015, **397**, 134.

152   S. He, C. M. Li, H. Chen, D. S. Su, B. S. Zhang, X. Z. Cao, B. Y. Wang, M. Wei, D. G. Evans and X. Duan, *Chem. Mater.*, 2013, **25**, 1040.

153   B. Y. Yu and I. L. Chien, *Ind. Eng. Chem. Res.*, 2015, **54**, 2339.

154   M. Gabrovska, R. M. E. Kardjieva, D. D. Crişan, P. Tzvetkov, M. Shopska and I. Shterewa, *React. Kinet. Mech. Cat.*, 2012, **105**, 79.

155   M. V. Gabrovska, R. M. Edreva-Kardjieva, D. D. Crişan, K. K. Tenchev, D. A. Nikolova and M. Crişan, *Bulg. Chem. Commun.*, 2013, **45**, 617.

156   S. H. Hwang, U. G. Hong, J. W. Lee, J. G. Seo, J. H. Baik, D. J. Koh, H. J. Lim and I. K. Song, *J. Ind. Eng. Chem.*, 2013, **19**, 2016.

157   D. C. Hu, J. J. Gao, Y. Ping, Li. H. Jia, P. Gunawan, Z. Y. Zhong, G. W. Xu, F. N. Gu and F. B. Su, *Ind. Eng. Chem. Res.*, 2012, **51**, 4875.

158   J. Carrasco, L. Barrio, P. Liu, J. A. Rodriguez and M. V. Ganduglia-Pirovano, *J. Phys. Chem. C*, 2013, **117**, 8241.

159   B. Sels, D. D. Vos, M. Buntinx, F. Pierard, A. K. D. Mesmaeker and P. Jacobs, *Nature*, 1999, **400**, 855.

160   A. Marimuth, J. W. Zhang and S. Lini, *Science*, 2013, **339**, 1590.

161   R. Neumann and M. Dahan, *Nature*, 1997, **388**, 353.

162   S. Linic and M. A. Barteau, *J. Am. Chem. Soc.*, 2003, **125**, 4034.

163   M. L. Bocquet, A. Michaelides, D. Loffreda, P. Sautet, A. Alavi and D.A. King, *J. Am. Chem. Soc.*, 2003, **125**, 5620.

164   S. Linic and M. A. Barteau, *J. Catal.*, 2003, **214**, 200.

165 D. Torres and F. Illas, *J. Phys. Chem. B*, 2006, **110**, 13310.

166 D. E. De Vos, J. Wahlen, B. F. Sels and P. A. Jacobs, *Synlett*, 2002, 367.

167 V. Rives and M. A. Ulibarri, *Coord. Chem. Rev.*, 1999, **181**, 61.

168 P. Liu, C. H. Wang and C. Li, *J. Catal.*, 2009, **262**, 159.

169 P. Liu, H. Wang, Z. C. Feng, P. L. Ying, C. Li, *J. Catal.*, 2008, **256**, 345.

170 Y. Y. Liu, K. Murata, T. Hanaoka, M. Inaba and K. Sakanishi, *J. Catal.*, 2007, **248**, 277.

171 B. M. Choudary, T. Ramani, H. Maheswaran, L. Prashant, K. V. S. Ranganath and K. V. Kumar, *Adv. Synth. Catal.*, 2006, **348**, 493.

172 M. P. Walsh, *SAE Paper*, 2001, **1**, 183.

173 P. Zelenka, W. Cartellieri and P. Herzog, *Appl. Catal., B,* 1996, **10**, 3.

174 Q. Wang, S. Y. Park, J. S. Choi and J. S. Chung, *Appl. Catal., B*, 2008, **79**, 101.

175 Q. Wang, S. Y. Park, L. Duan and J. S. Chung, *Appl. Catal., B*, 2008, **85**, 10.

176 C. M. L. Scholz, V. R. Gangwal, M. H. J. M. de Croon, J. C. Schouten, *J. Catal.*, 2007, **245**, 215.

177 H. Cheng, G. W. Cheng and H. D. Wang, *Chin. J. Catal.*, 2004, **25**, 272.

178 L. D. Li, J. J. Yu, Z. P. Hao and Z. P. Xu, *J. Phys. Chem. C*, 2007, **111**, 10552.

179 T. Y. Wang, Z. Lu, S. H. Yang and K. Sun, *Chem. Res.*, 2011, **27**, 734.

180 B. A. Silletti, R. T. Adams, S. M. Sigmon, A. Nikolopoulos, J. J. Spivey and H. H. Lamb, *Catal. Today*, 2006, **114**, 64.

181 L. Obalova, K. Karaskova, K. Jiratova and F. Kovanda, *Appl. Catal., B*, 2009, **90**, 132.

182 Z. P. Wang, Z. Jiang and W. F. Shangguan, *Catal. Commun.*, 2007, **8**, 1659.

183 Z. P. Wang, M. X. Chen and W. F. Shangguan, *Acta Phys. Chim. Sin.*, 2009, **25**, 79.

184 Z. P. Wang, Q. Li, L. G. Wang and W. F. Shangguan, *Appl. Clay. Sci.*, 2012, **55**, 125.

185 Z. Wang, Z. Zhang, H. Zhang, M. Chen and W. Shangguan, *J. Mol. Catal.*, 2007, **21**, PE-036.

186 J. J. Yu, Z. Jiang, S. F. Kang and Z. P. Hao, *Acta Phys. Chim. Sin.*, 2004, **20**, 1459.

187 S. F. Kang, J. H. Li and L. X. Fu, *Environ. Sci.*, 2007, **28**, 959.

188 A. E. Palomares, J. M. Lopez-Nieto, F. J. Lazaro, A. Lopez and A. Corma, *Appl. Catal., B*, 1999, **20**, 257.

189 F. F. Dai, M. Meng, Y. Q. Zha, Z. Q. Li, T. D. Hu, Y. N. Xie and J. Zhang, *Fuel Process. Technol.*, 2012, **104**, 43.

190 C. M. S. Polato, C. A. Henriques, A. C. C. Rodrigues and J. L. F. Monteiro, *Catal. Today*, 2008, **133-135**, 534.

191 W. P. Cheng, J. G. Yang, M. Y. He, *Catal. Commun.,* 2009, **10**, 784.

192 A. Corma, A. E. Palomares, F. Rey and F. Marquez, *J. Catal.*, 1997, **170**, 140.

193 G. Centi and S. Perathoner, *Appl. Catal., B*, 2007, **70**, 172.

194 A. J. Ragauskas, C. K. Williams, B. H. Davison, G. Britovsek, J. Cairney, C. A. Eckert, W. J. Frederick Jr, J. P. Hallett, D. J. Leak, C. L. Liotta, J. R. Mielenz, R. Murphy, R. Templer and T. Tschaplinski, *Science,* 2006, **311**, 484.

195 J. H. Clark, R. Luque and A. S. Matharu, *Ann. Rev. Chem. Biomol. Eng.,* 2012, **3**, 183.

196 J. Robert, *Plant Biotechnol. J.,* 2010, **8**, 288.

197 C. P. Pachpande and J. S. Waghmare, *Discovery Science*, 2013, **5**, 44.

198 J. B. Gonsalves, An Assessment of the Biofuels Industry in India in United Nations Conference on Trade and Development, 2006.

199 S. Carrettin, P. McMorn, P. Johnston, K. Griffin, C. J. Kiely and G. J. Hutchings, *Phys. Chem. Chem. Phys.,* 2003, **5**, 1329.

200 R. F. Stockel, *U.S. Pat.*, 086 977 A1, 2007.

201 S. K. Gupta, *U.S. Pat.*, 092 461 A1, 2007.

202 A. H. Rau, H. R. Renker and N. M. Quinn, *U. S. Pat.*, 0 003 675 A1, 2007.

203 A. Behr, J. Eilting, K. Irawadi, J. Leschinski and F. Lindner, *Green Chem.,* 2008, **10**, 13.

204 S. Carretin, P. McMorn, P. Johnston, K. Griffin and G. J. Hutchings, *Chem. Commun.*, 2002, 696.

205 A. Tsuji, A. Takagaki, K. Tirumal, V. Rao and K. Ebitani, *ChemSusChem,* 2011, **4**, 542.

206 M. N. Nadagouda and R. S. Varma, *Green Chem.,* 2006, **8**, 516.

207 K. Kaneda, K. Ebitani, T. Mizugaki and K. Mori, *Bull. Chem. Soc. Jpn.,* 2006, **79**, 981.

208 J. A. Dahl, B. L. S. Maddux and J. E. Hutchison, *Chem. Rev.,* 2009, **107**, 2228.

209 D. Tongsakul, S. Nishimura, C. Thammacharoen, S. Ekgasit and K. Ebitani, *Ind. Eng. Chem. Res.,* 2012, **51**, 16182.

210 D. Tongsakul, S. Nishimura and K. Ebitani, *ACS Catal.,* 2013, **3**, 2199.

211 A. Corma, S. Iborra and A. Velty, *Chem. Rev.*, 2007, **107**, 2411.

212 J. N. Chheda, G.W. Huber and J. A. Dumesic, *Angew. Chem., Int. Ed.*, 2007, **46**, 7164.

213 T. Werpy and G. Petoser, US Department of Energy report, 2004, http://www1.eere.energy.gov/biomass/pdfs/35523.pdf.

214 J. N. Chhed, G. W. Huber and J. A. Dumesic, *Angew. Chem., Int. Ed.*, 2007, **46**, 7164.

215 X. Tong, Y. Ma and Y. Li, *Appl. Catal., A*, 2010, **385**, 1.

216 N. K. Gupta, S. Nishimura, A. Takagaki and K. Ebitani, *Green Chem.*, 2011, **13**, 824.

217 A. Takagaki, M. Takahashi, S. Nishimura and K. Ebitani, *ACS Catal.,* 2011, **1**, 1562.

218 A. Gandini and N. M. Belgacem, *Polym. Int.,* 1998, **47**, 267.

219 M. Baumgarten and N. Tyutyulkov, *Chem. Eur. J.*, 1998, **4**, 987.

220 A. S. Amarasekara, D. Green, L. D. Williams, *Eur. Polym. J.,* 2009, **45**, 595.